



OPEN Synthesis, H₂S releasing properties, antiviral and antioxidant activities and acute cardiac effects of nucleoside 5'-dithioacetates

Miklós Bege^{1,2,3}✉, Miklós Lovas¹, Dániel Priksz⁴, Brigitta Bernát⁴, Ilona Bereczki^{1,5,6}, Rasha Ghanem Kattoub^{1,7}, Richárd Kajtár^{7,8}, Simon Eskeif^{7,8}, Levente Novák⁹, Jan Hodek¹⁰, Jan Weber¹⁰, Pál Herczegh¹, István Lekli⁸ & Anikó Borbás^{1,2,6}✉

Hydrogen sulfide (H₂S) is an endogenous gasotransmitter with cardioprotective and antiviral effects. In this work, new cysteine-selective nucleoside-H₂S-donor hybrid molecules were prepared by conjugating nucleoside biomolecules with a thiol-activatable dithioacetyl group. 5'-Dithioacetate derivatives were synthesized from the canonical nucleosides (uridine, adenosine, cytidine, guanosine and thymidine), and the putative 5'-thio metabolites were also produced from uridine and adenosine. According to our measurements made with an H₂S-specific sensor, nucleoside dithioacetates are moderately fast H₂S donors, the guanosine derivative showed the fastest kinetics and the adenosine derivative the slowest. The antioxidant activity of 5'-thionucleosides is significantly higher than that of trolox, but lower than that of ascorbic acid, while intact dithioacetates have no remarkable antioxidant effect. In human Calu cells, the guanosine derivative showed a moderate anti-SARS-CoV-2 effect which was also confirmed by virus yield reduction assay. Dithioacetyl-adenosine and its metabolite showed similar acute cardiac effects as adenosine, however, it is noteworthy that both 5'-thio modified adenosines increased left ventricular ejection fraction or stroke volume, which was not observed with native adenosine.

Keywords Nucleoside, Dithioacetate, H₂S donor, H₂S release kinetics, Antioxidant, Antiviral, SARS-CoV-2

Abbreviations

A	Adenine
ABTS	2,2'-azino-bis-(3-ethylbenzothiazoline-6-sulfonic acid)
Ac	Acetyl
Bu ₄ NBr	Tetrabutyl ammonium bromide
C	cytosine
DIAD	Diisopropyl azodicarboxylate
DMF	Dimethylformamide

¹Department of Pharmaceutical Chemistry, Faculty of Pharmacy, University of Debrecen, Egyetem tér 1, Debrecen 4032, Hungary. ²HUN-REN-UD Molecular Recognition and Interaction Research Group, University of Debrecen, Egyetem tér 1, Debrecen 4032, Hungary. ³Institute of Healthcare Industry, University of Debrecen, Nagyerdei krt. 98, Debrecen 4032, Hungary. ⁴Department of Pharmacology and Pharmacotherapy, Faculty of Medicine, University of Debrecen, Nagyerdei krt. 98, Debrecen 4032, Hungary. ⁵HUN-REN-UD Pharmamodul Research Group, University of Debrecen, Nagyerdei krt. 98, Debrecen 4032, Hungary. ⁶National Laboratory of Virology, University of Pécs, Ifjúság útja 20, Pécs 7624, Hungary. ⁷Doctoral School of Pharmaceutical Sciences, Faculty of Pharmacy, University of Debrecen, Nagyerdei krt. 98, Debrecen 4032, Hungary. ⁸Department of Pharmacodynamics, Faculty of Pharmacy, University of Debrecen, Rex Ferenc u. 1., Debrecen 4002, Hungary. ⁹Department of Physical Chemistry, Faculty of Science and Technology, University of Debrecen, Egyetem tér 1, Debrecen 4032, Hungary. ¹⁰Institute of Organic Chemistry and Biochemistry, Czech Academy of Sciences, Flemingovo nám. 2, Prague 166 10, Czech Republic. ✉email: bege.miklos@pharm.unideb.hu; borbas.aniko@pharm.unideb.hu

DPPH	2,2-Diphenyl-1-picrylhydrazyl
G	Guanine
HFIP	Hexafluoro isopropanol
HSAc	Thioacetic acid
MeOH	Methanol
MTT	3-(4,5-dimethylthiazol-2-yl)-2,5-(diphenyltetrazolium bromide)
NaOMe	Sodium methylate
PPh ₃	Triphenyl phosphine
TFA	Trifluoroacetic acid
THF	Tetrahydrofuran
TLC	Thin layer chromatography
Trt	Triphenylmethyl
TrtCl	Triphenylmethyl chlorid
Ts	<i>p</i> -toluenesulfonyl
TsCl	<i>p</i> -toluenesulfonyl chloride
TsOH	<i>p</i> -toluenesulfonic acid
U	Uridine

Hydrogen sulfide (H₂S) is known as a highly toxic foul-smelling compound, on the other hand, it is an important endogenous gasotransmitter, that plays a critical role in a wide range of biological processes¹. Endogenous H₂S is largely produced from cysteine and homocysteine as a metabolite of the transsulfuration pathway by the action of three enzymes, cystathionine β-synthase, cystathionine γ-lyase and 3-mercaptopyruvate sulfur transferase. H₂S is involved in several signaling pathways, including the regulation of cell proliferation by inducing apoptosis through increased p53 tumor suppressor gene expression². However, in some cell lines, such as endothelial cells, overproduction of H₂S can stimulate cell proliferation through kinase activation leading to angiogenesis³. Low H₂S levels can be observed in some neurological diseases (Parkinson's or Alzheimer's disease) demonstrating the neuromodulating effect of hydrogen sulfide⁴. H₂S has been shown to have anti-inflammatory and immunomodulating effects, and to protect against multiple stresses, including oxidative stress⁴⁻⁶. It can induce vasodilation by activating potassium channels⁷. H₂S shows significant activity against numerous fungi, including the human pathogen *C. albicans*⁸, and also inhibits the replication of a wide range of RNA viruses, such as the causative agent of COVID-19, SARS-CoV-2, presumably by preventing the pathogens from interacting with their receptors on the cell surface⁹⁻¹².

Based on these various biological effects, H₂S is a promising molecular entity in the prevention and treatment of several diseases. However, administering a highly toxic and extremely unpleasant-smelling gas poses a real challenge. Therefore, it is preferable to use H₂S donor molecules rather than hydrogen sulfide itself. The simplest of such compounds are inorganic sulfide, polysulfide and hydrogen-sulfide salts, although the H₂S releasing profile of these compounds is not ideal as they release a high amount of H₂S in a short period, causing short-lived effect¹³. To overcome this problem, several small-molecule organic H₂S donors have been developed that release hydrogen upon hydrolysis, endogenous triggers (usually thiols), or external stimuli^{13,14}. Some key representatives of organic H₂S donors include 1,2-dithiol-3-thiones, arylthioamides, aryl isothiocyanates and Lawesson reagent-based molecules such as GYY4137^{4,13-15}.

The hydrogen sulfide-releasing structures is often conjugated to nonsteroidal anti-inflammatory or other drugs or to different biomolecules to obtain H₂S-donor hybrid molecules that combine the beneficial therapeutic effects of the parent compound and H₂S¹⁶⁻¹⁹. Recently, we synthesized the H₂S-donor hybrid molecules **EV-34** and **BM-88** from the commonly used nonsteroidal anti-inflammatory drug ibuprofen (Fig. 1A), the former being a formaldehyde O,S-acylal, which is a hydrolysis-based H₂S donor^{14,20}, while **BM-88** is a dithioacetic acid ester that is activated by the endogenous trigger, cysteine²¹. We also produced a dithioacetate-containing H₂S donor hybrid, **BM-164**, from the well-known antioxidant ascorbic acid (vitamin C)²². All three compounds showed excellent hydrogen sulfide-releasing properties, and **BM-88** and **BM-164** also exhibited remarkable cardioprotective effects.

Nucleosides are important biomolecules, and their synthetic analogs are widely used in the anticancer and antiviral chemotherapy^{23,24}. Albeit sporadically, nucleosides have already been used to construct hydrogen sulfide donors, which always contain the H₂S-releasing group in the 5' position (Fig. 1B). Among them, compound **1** is an aryl-thioamide-type H₂S donor, which is connected to adenosine with a non-hydrolyzable ether bond²⁵, while derivatives **2** and **3** are nucleoside monophosphorothioates, which can be enzymatically converted into AMP and GMP, respectively, while hydrogen sulfide is released^{26,27}. Adenosine **1** significantly reduced infarct size when administered at the end of sustained ischemia and showed enhanced cardioprotection compared to adenine²⁵. Phosphorothioates **2** and **3** were reported to restore the anti-contractile effects of perivascular adipose tissue in obese rats through efficient H₂S release²⁶.

It is also worth mentioning that 5'-thio-modified nucleosides have significant bioactivity and therapeutic potential. Notably, 5'-thioadenosine derivatives exert significant antiprotozoal activity against *P. falciparum*^{28,29}, and 5'-thiothymidine was shown to be a strongly binding allosteric ligand of the SARS-CoV-2 NSP15 endonuclease³⁰. 5'-Cysteine and homocysteine derivatives of nucleosides and homonucleosides have been prepared and tested against S-adenosyl-homocysteine hydrolase and also used as monomer building blocks in the synthesis of peptide nucleic acids^{31,32}. Moreover, S-adenosylmethionine (SAM) is a well-known biomolecule that serves as a methyl donor in methyl transfer reactions³³.

Inspired by the literature results, we envisaged the synthesis of new cysteine-selective nucleoside-H₂S-donor hybrid molecules, which release H₂S in the body in a controllable manner, while being transformed into the corresponding 5'-thionucleoside (Fig. 1C). In this work, we describe the synthesis, H₂S-releasing and

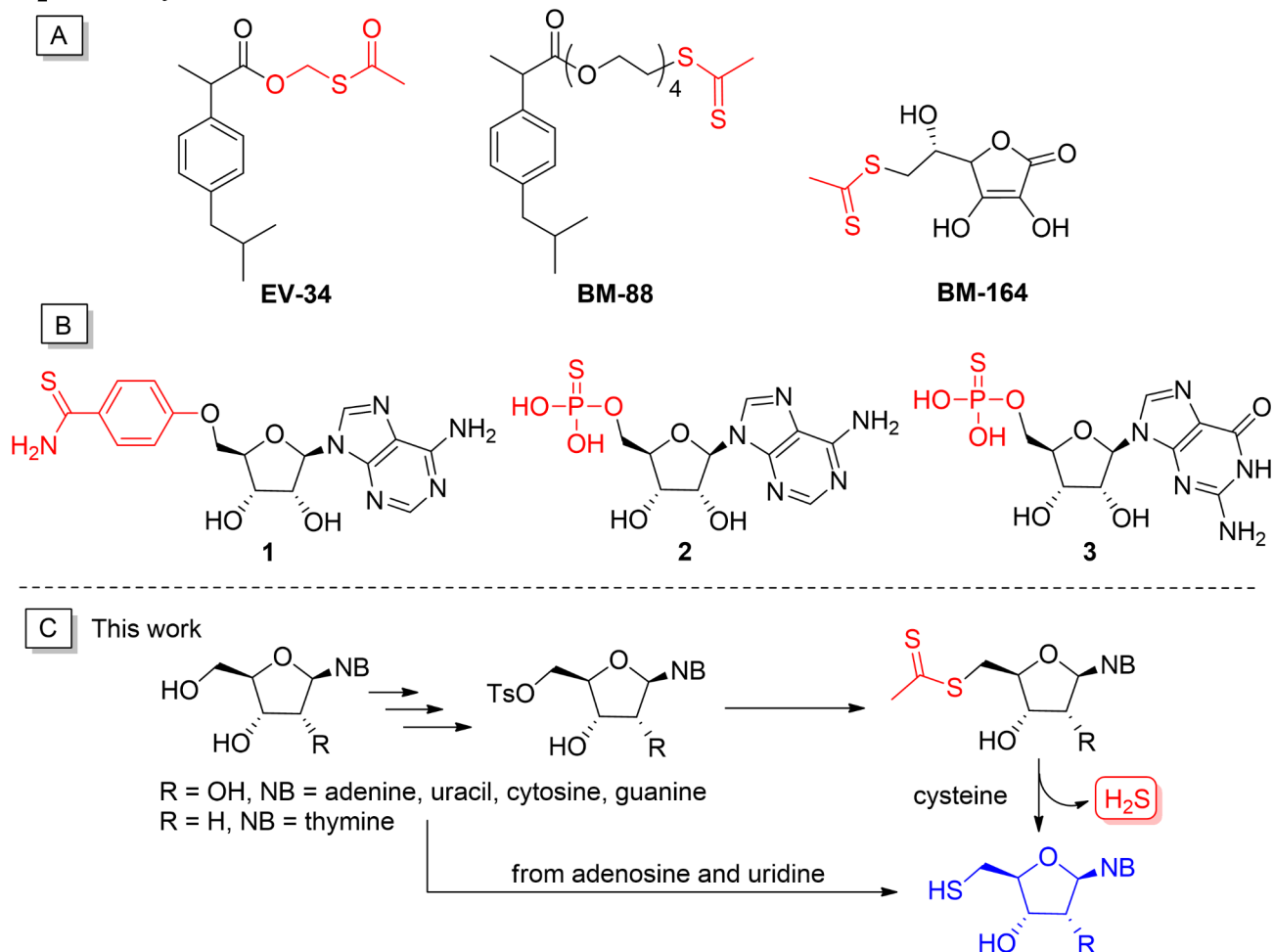
H₂S-donor hybrids in the literature

Fig. 1. (A) H₂S donors, previously synthesized by our research group; (B) H₂S donor nucleosides in the literature; (C) this work: synthesis and characterization of cysteine selective H₂S donor nucleosides and their metabolites.

antioxidant properties as well as antiviral effect against SARS-CoV-2 of the 5'-dithioacetate derivatives of the four canonical nucleosides (uridine, adenosine, cytidine, guanosine) and the deoxynucleoside thymidine. As reference compounds for the biological assays, the putative 5'-thio metabolites were also produced from uridine and adenosine. Given that adenosine plays a critical role in the regulation of heart function, we also studied the cardiac effects of the 5'-dithioacetyl adenosine derivative in a rat model.

Results and discussion

Synthesis

The synthesis of nucleoside 5'-dithioacetates was performed from properly protected nucleosides containing a leaving group in the 5'-position. Tosyl (Ts) was chosen as the leaving group, isopropylidene acetal was used to protect the 2' and 3' hydroxyl groups, while the exocyclic amino group of adenosine, guanosine and cytidine was protected with a triphenylmethyl (Trt) group (Fig. 2). Uridine was converted to 5'-tosylate **5** in two steps by isopropylideneation (**4**) followed by treatment with TsCl in pyridine³⁴. Adenosine, guanosine and cytidine were acetalated according to the literature method³⁵. Compounds **6**, **10** and **14** were O,N-ditritylated, followed by selective O-detritylation, using a cocktail of hexafluoroisopropanol (HFIP), and boron trifluoride diethyl etherate (BF₃·Et₂O) as Brønsted and Lewis acids, respectively, and triethylsilane (Et₃SiH) as reducing agent³⁶. The free 5'-OH of the resulting **8**, **12** and **16** was tosylated to obtain the fully protected 5'-tosylates **9**³², **13** and **17**.

The required tosylate was prepared from the deoxynucleoside thymidine in one step without the use of any protecting group. By reacting thymidine with TsCl in pyridine at room temperature, only the 5',3'-ditosylate was obtained. Repeating the reaction at 0 °C, the desired 5'-O-monotosyl derivative (**18**)³⁷ was formed as the main product.

Next, the dithioacetate group was introduced into the 5'-position of the nucleoside using a one-pot reaction. First, the Mg salt of dithioacetic acid was produced in situ by the reaction of carbon disulfide and methyl magnesium bromide, using a modified version of the method described by Maeda et al.³⁸ (Fig. 3A).

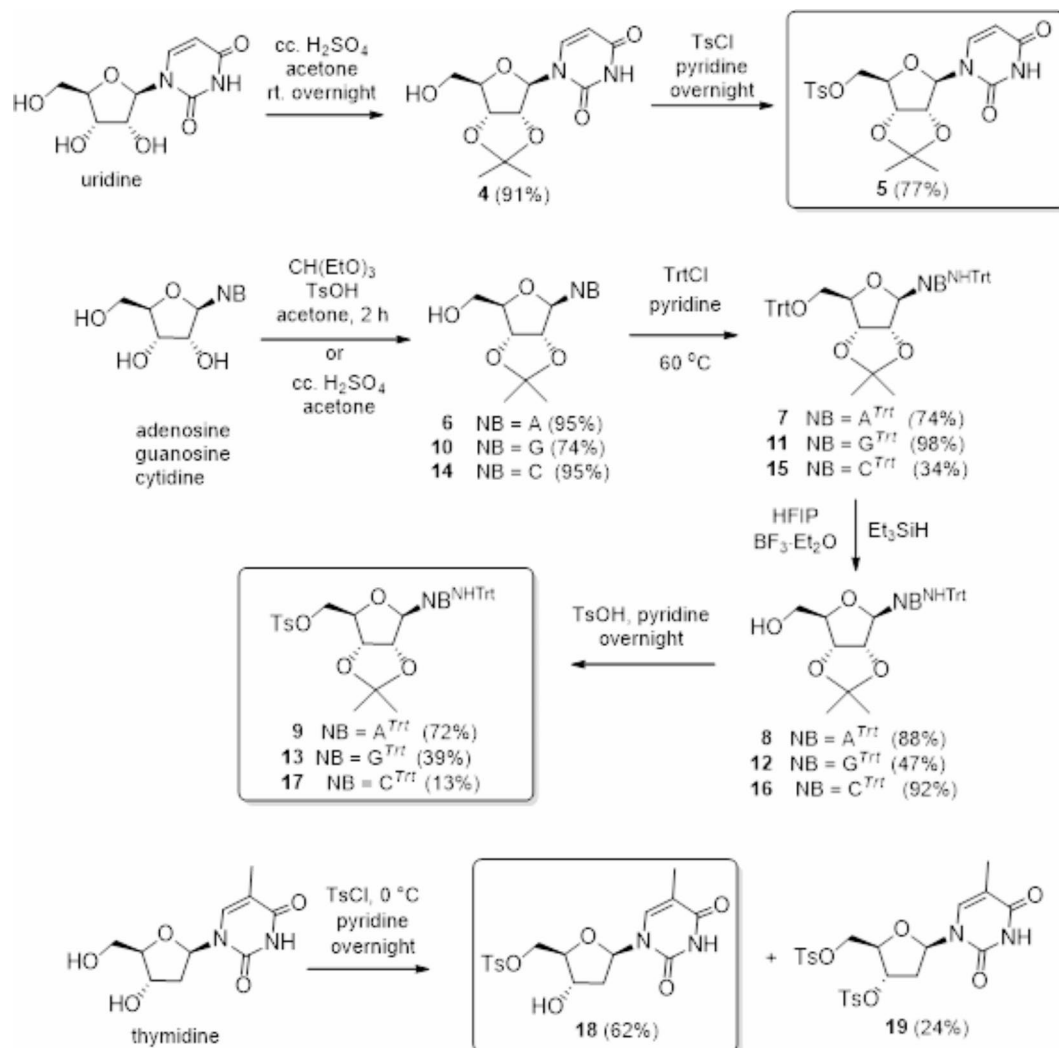


Fig. 2. Synthesis of nucleoside 5'-tosylates.

Nucleoside tosylate was then added to the reaction mixture and reacted with the dithioacetate at 80 °C. After 5 h, completion of the reaction and the formation of a uniform product was observed by TLC. Unfortunately, however, NMR spectra showed that the chromatographically uniform product was an inseparable 1:1.4 mixture of the desired 5'-dithioacetate (**21**) and a side product. We assumed that 5'-deoxy-5'-bromouridine (**20**) is formed as an undesired product, and to prove this, the presumed bromo derivative was synthesized from **5**, using tetrabutylammonium bromide at 80 °C. By comparing the NMR spectra of the obtained 5'-bromouridine **20** and the mixture (Fig. 3B), it was confirmed that the impurity is indeed the 5'-bromo derivative. The rapid conversion of tosylate to bromouridine (2.5 h) and the high proportion of the latter in the mixture after 5 h indicate that the bromo derivative is formed first, which is converted to dithioacetate in a slow reaction. Accordingly, the reaction was repeated with an extended reaction time of 18 h. In this case, only the desired 5'-dithioacetate was obtained with good yield (80%).

Based on the above, nucleoside 5'-tosylates **9**, **13**, **17** and **18** were reacted with 3 equiv. of dithioacetate salt in an 18-hour reaction at 80 °C to obtain the desired **23**, **28** and **30**. In the case of the guanosine derivative, only the 5'-bromoderivative **25** was formed under the above conditions, which could be converted to the desired **26** in 85% yield with a large excess of dithioacetate salt during a 28-hour reaction. Adenosine dithioacetate **23** was formed with $\text{CH}_3\text{CSSMgBr}$ in an exceptionally low yield of 28%, which significantly increased to 72% when the reaction was performed with potassium dithioacetate obtained in two steps from the magnesium salt.

The trityl and isopropylidene protecting groups were removed in one step with 90% trifluoroacetic acid, using triethylsilane as a reducing agent in the presence of trityl group (Fig. 4A).

It is assumed, that in a biological milieu, the synthesized 5'-dithioacetyl nucleosides are converted to the corresponding 5'-thionucleosides triggering by the endogenous thiol cysteine. Thus, the assumed metabolites of 5'-dithioacetyl-adenosine and -uridine were also synthesized for biological study. Uridine and adenosine were converted into 5'-acetylthio derivatives **31** and **33** in a Mitsunobu-like reaction, then the S-acetyl group was cleaved, using sodium methylate to obtain the desired thiols **32** and **34** in good yields (Fig. 4B).

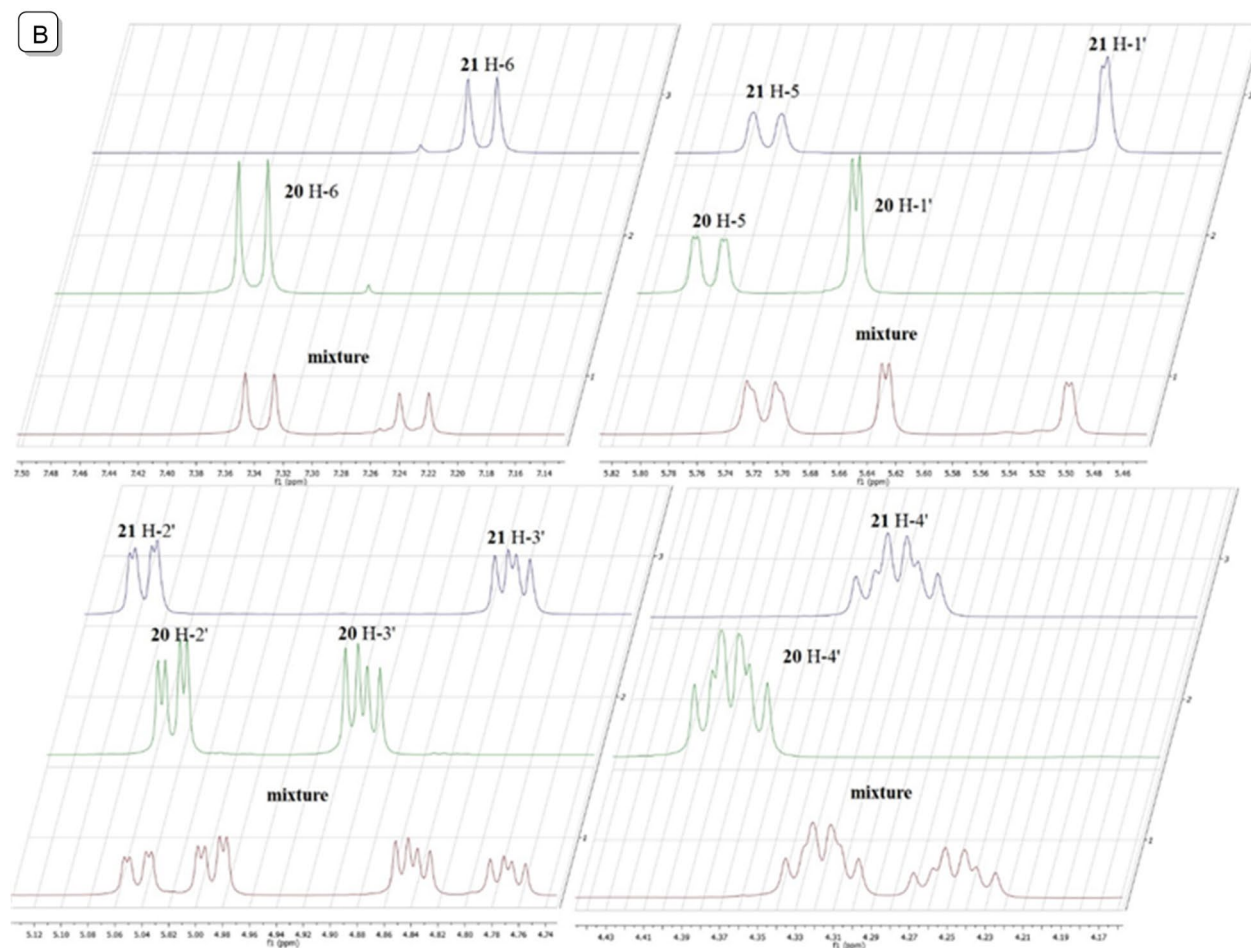
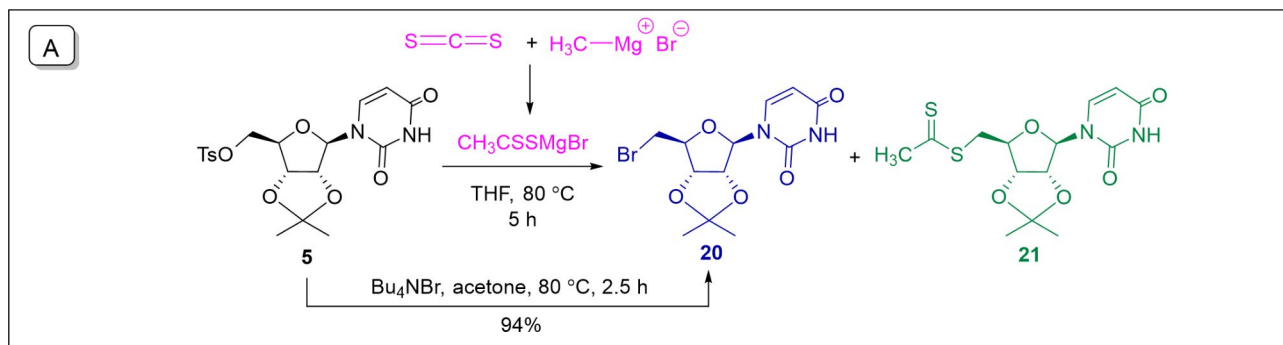


Fig. 3. (A) Synthesis of the uridine dithioacetate **21** by freshly prepared dithioacetate salt $\text{CH}_3\text{CSSMgBr}$; (B) Comparison of the characteristic NMR signals of the ^1H spectra of dithioacetate **21**, bromouridine **20** and their mixture.

Evaluation of H_2S releasing profile of the compounds

The H_2S release of compounds **22**, **24**, **27**, **29** and **30** was detected in Dulbecco's modified Eagle's medium with an amperometric, H_2S -specific sensor. The gas release reached the maximum level after 10–20 min and remained at a measurable level even after two hours. On the other hand, the base clearly also has a role in the kinetics of the process. The guanosine derivative **27** releases a large amount of H_2S relatively quickly, while adenosine and thymidine release H_2S more slowly than the other nucleosides, and adenosine has the longest-lasting effect (Fig. 5A–E). We also studied the H_2S emissions of two known H_2S donors as references, the fast-release NaHS and the slow-release GYY4137 (Fig. 5F). With the latter, there was no measurable H_2S release, which is in line with the literature data, according to which GYY4137 requires the presence of a high concentration of cysteine (4 mM) for detectable generation of H_2S ⁷. Based on the comparison with the reference compounds, it can be concluded that nucleoside dithioacetates can be considered H_2S donors with a medium release rate.

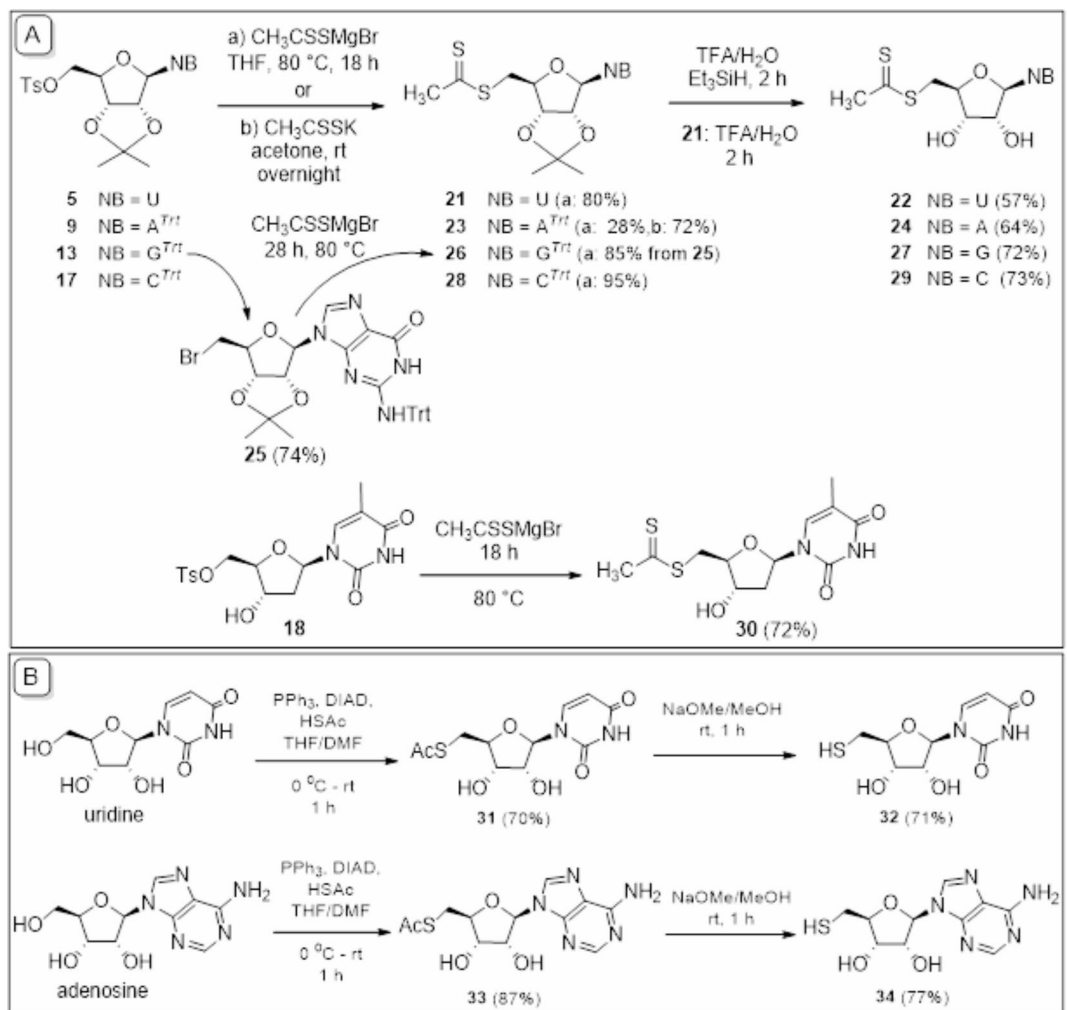


Fig. 4. (A) Synthesis of nucleoside dithioacetates **22**, **24**, **27**, **29** and **30**; (B) synthesis of 5'-thionucleosides **32** and **34**.

Based on literature results, H_2S is released from dithioester derivatives via a native chemical ligation mechanism mediated by cysteine (Fig. 5G, route a), resulting in thiol (**II**), cysteine-derived dihydrothiazole (**V**) and H_2S ²¹. This mechanism is unlikely to be influenced by the structure of the nucleosides. However, Liu and Orgel showed that dithioacetates can undergo hydrolysis catalyzed by native aspecific esterases²⁰. In this reaction pathway, in addition to the thiol, a thioacetic acid is formed, which spontaneously oxidizes to disulfide (**VIII**), and finally the disulfide reacts with native amines to produce acetamide and H_2S (Fig. 5G, route b). The structure of the nucleosides certainly influences this enzyme-catalyzed process, which is likely to account for the slightly different kinetics of hydrogen sulfide release for different nucleoside structures.

Antioxidant assays

Oxidative stress arises from an imbalance between increased reactive oxygen species (ROS) production and diminished antioxidant host defenses. Growing evidence suggests that this condition significantly contributes to the pathogenesis of several human diseases, including SARS-CoV-2 infection³⁹. With the 5'-dithioacetate derivatives and their synthetic 5'-SH metabolites in hand, the antioxidant activities of compounds **22**, **24**, **32**, and **34** were estimated in the DPPH radical scavenging assay. Furthermore, the ability of the two former dithioacetate derivatives, as well as the H_2S -donor GYY4137 serving as a positive control, was also evaluated after the addition of a homogenized rat heart extract.

As mentioned above, our newly designed compounds are H_2S donor nucleoside derivative prodrugs featuring a dithioacetate moiety. These prodrugs undergo cysteine-mediated transesterification²¹ or aspecific esterase-catalyzed hydrolysis²⁰, resulting in the release of H_2S and the corresponding 5'-thionucleoside. In the present study, we utilized a freshly prepared supernatant obtained from the tissue homogenate of a frozen control rat heart in PBS buffer to replicate physiological conditions, thus inducing H_2S release.

Endogenous antioxidants play a crucial role in enhancing cellular defense against the harmful effects of reactive oxygen species (ROS)⁴⁰. The presence of these antioxidants in the extract used in our study may lead to misinterpretations of the radical scavenging efficacy of the compounds under investigation. To prevent such

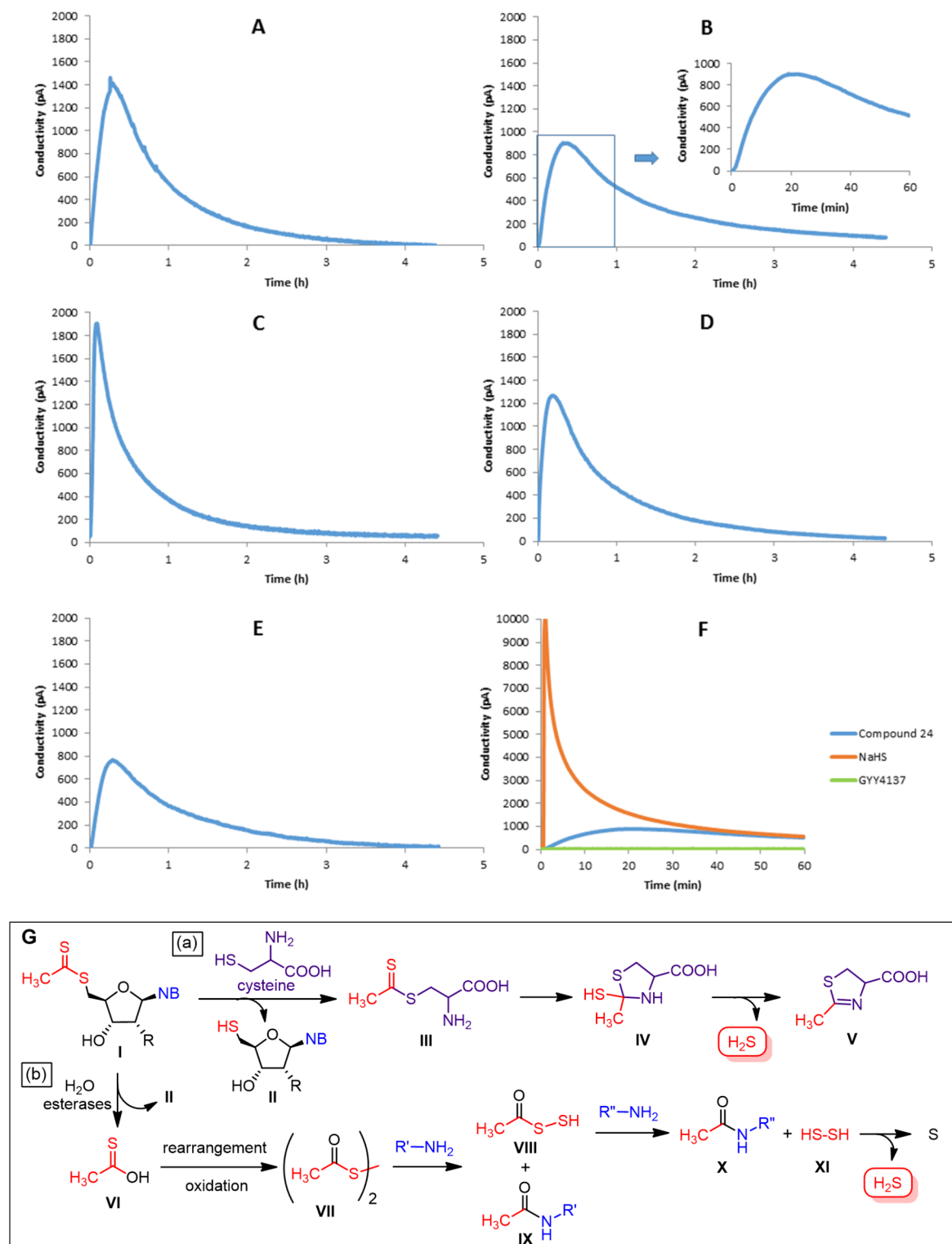


Fig. 5. H₂S releasing curves measured by H₂S selective sensor (A–F, 10% w/v) and two possible routes of H₂S release from 5'-dithioacetyl nucleosides under physiological conditions (G). (A) Compound 22 (0.31 mM); (B) compound 24 (0.29 mM) (inset: first 60 min); (C) compound 27 (0.28 mM); (D) compound 29 (0.32 mM); (E) compound 30 (0.32 mM); (F) the blue curve shows the H₂S release of compound 24 (0.31 mM), the orange curve shows the H₂S release of NaHS (0.1 mg in 5 mL of distilled water, 0.36 mM) and the green curve shows the H₂S release of GYY4137 (0.5 mg in 5 mL of medium, 0.27 mM); (G) H₂S release (a) by cysteine-mediated transesterification, (b) by aspecific esterase-catalyzed hydrolysis.

interference, the extract can only be introduced in a volume that shows no or negligible radical scavenging ability. Therefore, we tested different volumes of the extract, ranging from 50 to 5 μL , in a 200:800:1000 μL mixture of methanol, 0.1 M Tris-HCl buffer, and DPPH. The measurements were carried out immediately and after 30 min of incubation, ensuring no time-dependent behavior. The extract demonstrated inhibition ratios of 6% and 15% against the DPPH \cdot free radical when 25 μL of the extract was utilized immediately and after a 30-minute incubation period, respectively. Conversely, extract volumes ranging from 20 μL to 5 μL yielded minimal scavenging ratios of only 1.5% and 2.5%, immediately and after 30 min of incubation, respectively. Therefore, the highest volume, 20 μL , which exhibited no activity at either time point was selected for further experimentation (Fig. S1).

The resulting inhibition ratios of the compounds tested were then compared with those obtained for the precursor uridine or adenosine, as well as the positive controls. Three positive controls were employed in this study: 0.5 mM ascorbic acid solution, along with two H₂S-releasing molecules — sodium hydrosulfide (NaHS), which releases H₂S rapidly, and the slow-releasing organic H₂S donor GYY4137.

Figure 6 depicts the correlations between the concentrations (mM) and DPPH inhibition ratios (%) of the compounds tested immediately and after 30 min of incubation. Remarkable differences in the inhibition ratios were observed in both time- and concentration-dependent manners.

As shown in Fig. 6, immediate antioxidant activity was observed in all compounds. The 5'-SH metabolites **32** and **34** demonstrated notably higher antioxidant activity than the corresponding 5'-dithioacetate derivatives (**22** and **24**), achieving an inhibition ratio of 70–80% and 90% immediately and after 30 min incubation, respectively, when employed at a concentration of 2 mM.

0.5 mM NaHS or GYY4137 resulted in the release of detectable amounts of H₂S, as evidenced by their DPPH inhibition ratios recorded immediately and after a 30-minute incubation period. The release of H₂S from NaHS occurred rapidly, reaching a DPPH inhibition ratio of 90% at the 30-minute mark. In contrast, the release of H₂S from GYY4137 was significantly lower, but sustained throughout the incubation duration, as demonstrated by the increase in the inhibition ratio.

Notably, the dithioacetate derivatives **22** and **24** with 20 μL of the homogenized myocardial extract showed a higher antioxidant activity than without the extract, and surpassed that of the 5'-SH metabolite at lower concentrations after 30 min of incubation, clearly demonstrating that the DPPH inhibitory activity of the

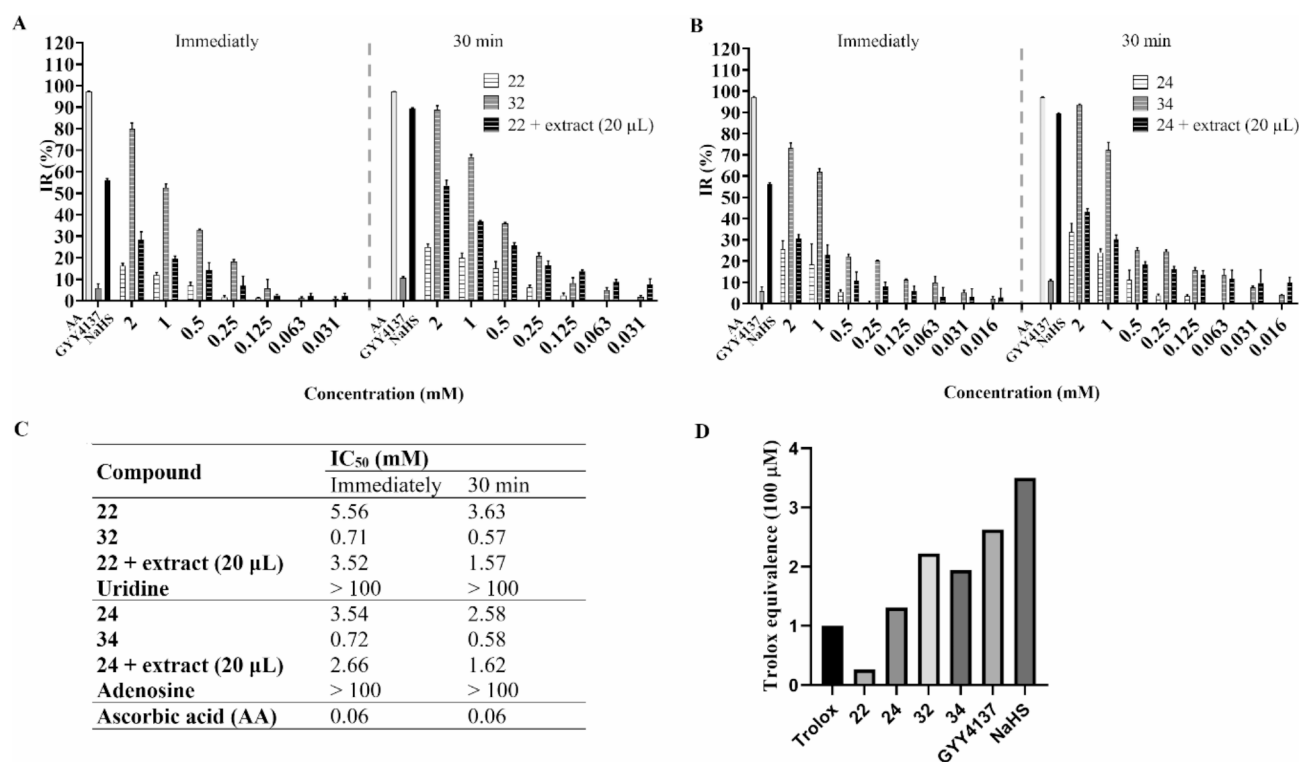


Fig. 6. DPPH inhibition ratio of (A) compounds **22**, **32**, and **22 + extract (20 μL)**, and (B) compounds **24**, **34**, and **24 + extract (20 μL)** immediately and after 30 min of incubation, compared to the positive controls (0.5 mM ascorbic acid (AA), IR = 97.25% and 97.13%), 0.5 mM GYY4137 (IR = 5.95% and 10.63%), and 0.5 mM NaHS (IR = 56.14% and 90.03%), immediately and after 30-min incubation, respectively). Error bars symbolize the standard deviation from the mean value ($n = 3$). Results express mean \pm SD. IR = inhibition ratio. (C) IC₅₀ values (mM) of synthetic compounds compared to the corresponding nucleosides and ascorbic acid (AA). (D) ABTS (2,2'-azinobis-(3-ethylbenzothiazoline-6-sulfonic acid) radical cation decolorization assay of compounds **22**, **24**, **32**, **34**, GYY4137, and NaHS. Values are expressed as Trolox equivalents (a vitamin E analogue). Error bars symbolize the mean \pm SEM ($n = 9$).

dithioacetate derivatives in the presence of the extract continuously increases during the 30-min incubation time due to the sustained concurrent release of two antioxidant molecules: the 5'-SH metabolite and H₂S.

The IC₅₀ values of the synthesized compounds deviated significantly from that belonging to the reference compounds, with the 5'-SH analogues **32** and **34** as the most active. However, the observed activity was 10 times lower than that achieved with ascorbic acid.

It should be noted that 20 µL triggering extract was also introduced to the vitamin C and compounds **24** and **34** groups. The degree of discoloration of the free radical was monitored over a duration of 30 min. The extract demonstrated negligible or only minimal negative effects on the inhibition ratios of these groups, which were primarily noted at high concentrations. This finding indicates that the extract acts mainly on the dithioacetate group.

Furthermore, we compared the antioxidant activity of dithioacetate derivatives and 5'-SH metabolites using ABTS (2,2'-azinobis-(3-ethylbenzothiazoline-6-sulfonic acid)) assay, which showed a similar activity pattern to the DPPH assay. Among the molecules the 5'-SH metabolites **32** and **34** showed higher antioxidant activity than the parent dithioacetate derivatives **22** and **24**. (Fig. 6, panel D).

Cell viability

In order to evaluate the biocompatibility of the new compounds, MTT assays were carried out in the presence of different concentrations of 5'-dithioacetate derivatives and their synthetic 5'-SH metabolites on H9c2 cells. None of the molecules showed cell toxicity in a physiologically relevant concentration range (Fig. S2).

Antivirals results

To determine H₂S releasing effect of nucleoside 5'-dithioacetates on SARS-CoV-2 replication, we added compounds to Calu-3 lung epithelial cells two hours after infection and washing virus away. As the release of H₂S is relatively short-lived we evaluated anti-SARS-CoV-2 effect of compounds already two days after infection in cytopathic-effect-based assay using sensitive CellTiter-Glo luminescent cell viability assay. Only compounds **24** and **27** exhibited moderate anti-SARS-CoV-2 activity in Calu-3 cells with an EC₅₀ of 173 ± 24 µM and 158 ± 34 µM, respectively (Table 1). Next, the virus yield reduction assay was performed to ascertain if there is direct effect on the released SARS-CoV-2 virions into media. The medium after two days infection of Calu-3 cells was analyzed in Vero E6 cells using plaque assay. Only compound **27** very slightly reduced the SARS-CoV-2 titer by 0.38 log₁₀ PFU/mL.

Results of in vivo experiments

The cardiac effects of 5'-dithioacetyl uridine and adenosine (**22** and **24**), 5'-thioadenosine (**34**) and adenosine as a reference compound were evaluated in rat model. Adenosine at a dose of 2 mg/kg induced heart block, and heart rate (HR) remained significantly lower 30 s post-administration compared to baseline; however, this negative chronotropic effect dissipated within approximately 60 s. None of the new compounds (**22**, **24**, and **34**) induced complete heart block or pauses, but adenosine derivatives **24** and **34** significantly reduced HR relative to baseline values ($p=0.0162$; and $p=0.0010$, respectively). Although the negative chronotropic effect of compounds **24** and **34** was less pronounced than that of adenosine, their duration of action was longer. The uridine-based compound **22** did not produce notable changes in HR, though a non-significant reduction was observed ($p=0.0562$).

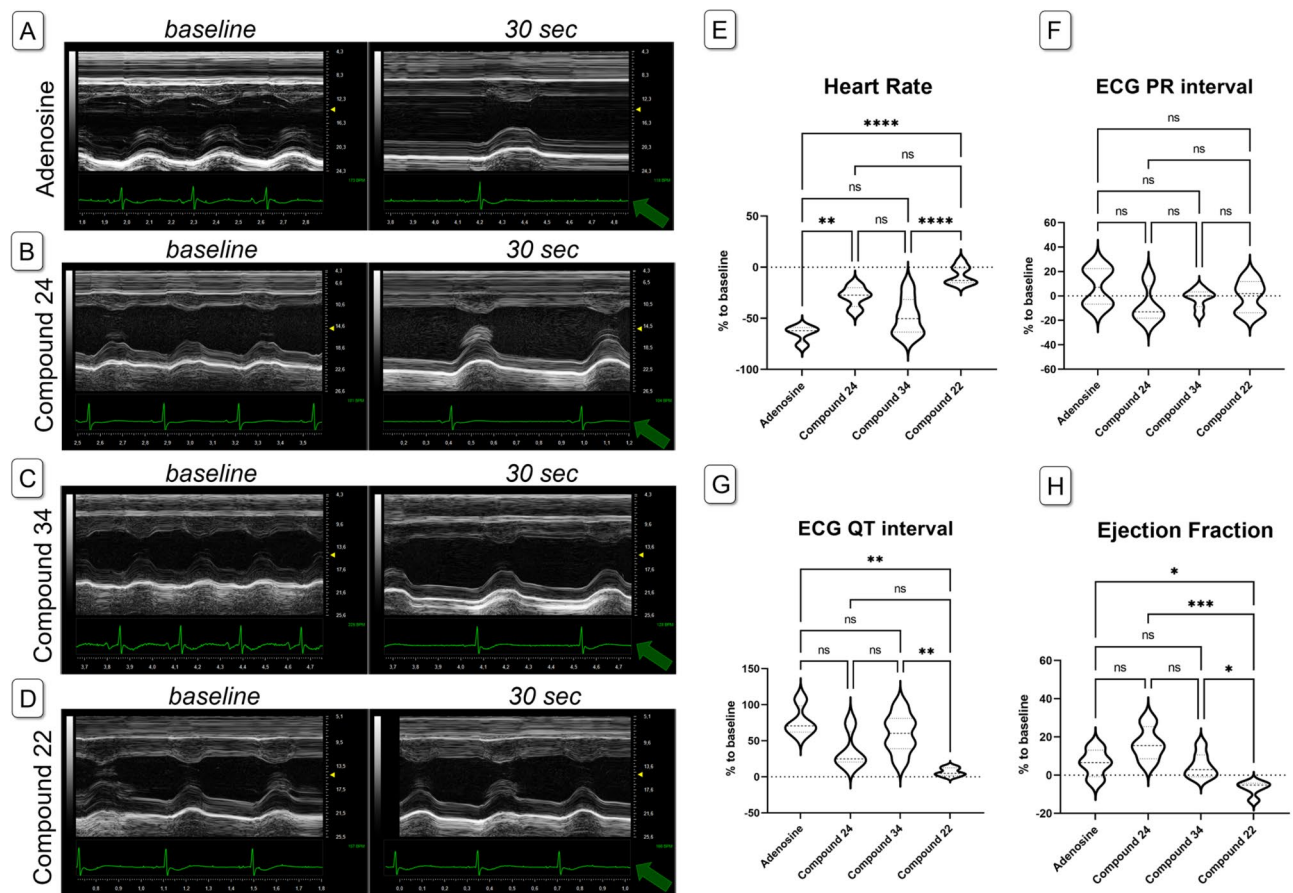
Neither the new compounds nor adenosine significantly affected the ECG PR interval in anesthetized rats. Adenosine significantly prolonged the QT interval ($p=0.0062$ vs. baseline), and both compounds **24** and **34** similarly extended the QT interval compared to their corresponding baseline values ($p=0.0035$ and $p=0.0034$, respectively), akin to the parent compound adenosine. Compound **22** did not alter PR or QT intervals but slightly decreased ejection fraction (EF) 30 s after administration ($p=0.0208$ vs. baseline). Adenosine and compound **34** tended to increase EF ($p=0.189$ and $p=0.0757$ vs. baseline, respectively), whereas compound **24** significantly increased EF ($p=0.0302$ vs. baseline). Interestingly, stroke volume (SV) remained unchanged following administration of adenosine or compound **22**, but both compounds **24** and **34** increased SV ($p=0.0811$ and $p=0.0068$, respectively; Fig. 7).

Conclusions

By optimizing the synthesis steps, we developed an efficient route for the synthesis of new hydrogen sulfide donor nucleosides containing a dithioacetyl group. Using amperometric, H₂S-specific sensor measurements, we established that dithioacetate nucleosides are medium-speed H₂S donors, and nucleobases also have an effect on

Compound	EC ₅₀ ± SE [µM]	CC ₅₀ ± SE [µM]	SARS-CoV-2 titer reduction [log ₁₀ PFU/mL]
22	> 1000	> 1000	0.02
24	173 ± 24	~ 1000	0
27	158 ± 34	> 1000	0.38
29	> 1000	> 1000	0.13
30	621 ± 181	764 ± 82	0.01
Remdesivir	0.5 ± 0.26	> 10	7.1

Table 1. Anti-SARS-CoV-2 activities (EC₅₀), cytotoxicity in Calu-3 cells (CC₅₀) and virus yield reduction assay for nucleoside 5'-dithioacetates.



the kinetics of hydrogen sulfide release. DPPH and ABTS assays were used to determine the antioxidant profile of the hydrogen sulfide donor uridine and adenosine and their 5'-thio metabolites.

In the antiviral tests against SARS-CoV-2, both adenosine and guanosine derivatives **24** and **27** showed an antiviral effect, but surprisingly, only the fastest hydrogen sulfide-releasing guanosine derivative **27** measurably reduced the virus titer. According to literature results, H₂S can suppress infections caused by enveloped viruses, including SARS-CoV-2, through several mechanisms, one of the most important of which is the induction of long-term antioxidant activity^{11,41}. H₂S can directly activate the Nrf2 transcription factor pathways, and also contributes to antioxidant activity through various indirect effects, such as maintaining increased levels of an important antioxidant compound, glutathione^{41,42}. Glutathione has been shown to have therapeutic potential against COVID-19, being able to reduce disulfide bonds in the SARS-CoV-2 spike protein and its human receptor ACE-2, which disrupts the spike protein ACE2 interaction, preventing viral entry^{43,44}. Until now, mostly slow-release hydrogen sulfide donors (e.g. Na₂S₂O₃ and GYY4137) have been shown to have anti-SARS-CoV-2

◀ **Fig. 7.** Comparison of the cardiac effects of adenosine ($n=4$), compound **24** ($n=4$), **34** ($n=7$) and **22** ($n=5$) on anaesthetized SD rats. Panels (A–D) show M-mode traces of the left ventricle, obtained from PSAX view at baseline and 30 s after drug administration (sweep speed adjusted to 60 0 Hz). Compound **24** and **34** caused similar but smaller effect than the parent molecule adenosine. Ejection fraction (panel H) increased after compound **24** administration but slightly decreased under the influence of compound **22**. Heart rate decreased after adenosine, compound **24** and **34** administration, but only slightly changed after compound **22** injection (panel E). ECG PR interval was unchanged in all cases (panel F). A significant QT interval prolongation on the ECG was observed after the administration of all adenosine-based compounds, but not after the uridine-based (panel G). One-way ANOVA with Tukey post-test was used to compare % changes of the parameters in the treatment groups. Asterisks denote the level of significance: * $p < 0.05$; ** $p < 0.01$; *** $p < 0.001$. Green arrows denote lead II ECG traces. Panel (I) Effect of adenosine, compound **24**, **34** and **22** on ECG and echocardiographic parameters, at the baseline and 30 s after i.v. drug administration (2 mg/kg, i.v.). Adenosine-based compounds significantly decreased heart rate with a marked QT prolongation, while increased SV and EF. All data is presented as mean \pm SD. Asterisks denote the level of significance: * $p < 0.05$; ** $p < 0.01$; *** $p < 0.001$ (paired t-test, vs. baseline values).

effects^{9–11}, but the role of the hydrogen sulfide release rate in the antiviral effect has not been investigated. Therefore, literature results do not provide evidence that the antiviral activity of the guanosine derivative **27** is related to its slightly faster sulfide-releasing kinetics compared to other nucleosides or is due to other factors, which requires further investigation.

In the *in vivo* experiments, administration of 2 mg/kg adenosine resulted in a significant reduction in heart rate (negative chronotropy) accompanied by a marked prolongation of the ECG QT interval, consistent with literature reports^{45,46}. Interestingly, the effects of the novel adenosine-based compounds **24** and **34** were less pronounced in terms of negative chronotropy and QT prolongation when administered at the same dose (2 mg/kg). However, the heart rate-lowering effect of compound **34** did not significantly differ from that of adenosine. Notably, the duration of the negative chronotropic effect was longer for compounds **24** and **34** compared to the parent compound. The ECG PR interval, indicative of AV nodal conduction, remained unchanged following drug administration. The uridine-based compound **22** produced a non-significant reduction in heart rate without altering other ECG parameters. Regarding left ventricular systolic parameters, compound **22** slightly decreased ejection fraction. Interestingly, both compounds **24** and **34** increased left ventricular ejection fraction and stroke volume, an effect not observed with adenosine. Adenosine induced heart block but did not significantly affect ejection fraction or stroke volume during the rapid recovery phase, consistent with existing literature⁴⁷. This phenomenon can be explained by the interplay of two effects: the bradycardic effect, which enhances ventricular filling and subsequently increases stroke volume via the Frank-Starling mechanism, and the minimal negative inotropic effects of adenosine, which result in a relatively unchanged ejection fraction when these effects are considered together. In addition, previous *in vivo* studies have also shown that adenosine alone does not alter ventricular contractility, corroborating our current findings⁴⁸. Additionally, the bradycardic action of adenosine dissipated rapidly (in seconds), further elucidating the non-significant increases observed in ejection fraction and stroke volume. In contrast, the more pronounced increases in stroke volume and ejection fraction associated with the adenosine-based compounds **24** and **34** may be attributed to a more long-lasting reduction in heart rate. During physiological conditions, the Frank-Starling mechanism allows the heart to maintain cardiac output by increasing stroke volume at lower heart rates; thus, we propose that in the case of these two adenosine derivatives, the Frank-Starling mechanism is the predominant factor. Furthermore, according to literature, the release of hydrogen sulfide (H_2S) demonstrates vasodilatory effects, potentially contributing to enhanced cardiac blood flow, increased venous return, and subsequent improvements in ejection fraction (EF) and stroke volume (SV)⁴⁹. These effects, however, were not observed with the uridine-based compound **22**, which releases H_2S rapidly (based on our current data) but probably lacks binding affinity for adenosine receptors⁵⁰. This distinction was evident in our *in vivo* findings, where compound **22** did not significantly influence heart rate, atrioventricular (AV) nodal conduction, SV, or EF. Based on these results, we hypothesize that the observed alterations in EF and SV with adenosine-based compounds are likely secondary to the bradycardia elicited by their mechanism of action, consistent with the effects of the parent molecule, adenosine. Future research could involve a more detailed mechanistic evaluation, examining the compound's effects at varying doses and dosing intervals while employing specific inhibitors of adenosine receptors and transporters. The distinct cardiac effects associated with adenosine-based compounds underscore the need for further investigation to elucidate their mechanisms and potential therapeutic applications.

Experimental methods

General informations

Compounds **5**³⁴, **9**³², **10**³⁵, **14**³⁵ and **18**³⁷ were prepared according to literature procedures. Nucleosides and reagents were purchased from Sigma-Aldrich Chemical Co. and used without further purification. The optical rotation values of the nucleoside derivatives were determined on a Perkin-Elmer 241 automatic polarimeter. The reactions were monitored by thin-layer chromatography (TLC) on Kieselgel 60 F254 (Merck), detection was done with UV light (254 nm) and by immersion in sulfuric acid ammonium molybdate solution or 5% ethanolic sulfuric acid, followed by heating. Purification was performed by flash chromatography on a silica gel 60 column (Merck, 0.040–0.063 mm). The organic solutions were dried over anhydrous Na_2SO_4 or $MgSO_4$, and solvents were evaporated *in vacuo*. The NMR and MS analysis of the compounds was performed as previously described^{32,34}. Briefly, 1H NMR (360 and 400 MHz) and ^{13}C NMR (90 and 100 MHz) spectra were

recorded with Bruker DRX-360 and Bruker DRX-400 spectrometers at 25 °C, chemical shifts are referenced to Me₄Si (0.00 ppm ¹H) and residual solvent signals (CDCl₃: 77.2, DMSO-d₆: 39.5, CD₃OD: 49.0 for ¹³C). Two-dimensional COSY and ¹H-¹³C HSQC experiments were used to assist NMR assignments. MALDI-TOF MS analyses of the compounds were carried out in the positive reflectron mode using a Bruker Autoflex Speed mass spectrometer equipped with a time-of-flight (TOF) mass analyzer (Bruker, Germany). 2,5-Dihydroxybenzoic acid (DHB) was used as matrix and F₃CCOONa as cationising agent in DMF.

Synthesis of the compounds

2',3'-O-Isopropylidene-5'-O-tosyl-2-N-trityl-guanosine (13): Compound **12** (1.5 g, 2.65 mmol) was dissolved in dry pyridine (20 mL), TsCl (657 mg, 3.45 mmol, 1.3 equiv.) was added and stirred at rt overnight. Because of the low conversion, another portion of TsCl (657 mg, 3.45 mmol, 1.3 equiv.) was added and stirred for another night. Next day, the reaction mixture was evaporated, the residue was dissolved in CH₂Cl₂ (350 mL) and extracted with 10% aq. Na₂HSO₄ solution and brine. The organic phase was dried over Na₂SO₄, filtered and evaporated under reduced pressure. The crude product was purified by flash column chromatography (gradient elution CH₂Cl₂/MeOH 98:2 → 97:3 → 95:5) to give **13** (558 mg, 29%) as a white foam. [α]_D²⁰ = +19.05 (c=0.21, CHCl₃), Rf=0.17 (CH₂Cl₂/MeOH 95/5), ¹H NMR (400 MHz, CDCl₃) δ (ppm) 7.77 (s, 1 H), 7.64 (d, J=8.3 Hz, 2 H), 7.29 (dd, J=15.7, 7.8 Hz, 8 H), 7.12 (dt, J=23.7, 7.1 Hz, 9 H), 6.96 (s, 1 H), 5.36 (d, J=2.1 Hz, 1 H), 4.85–4.80 (m, 1 H), 4.18 (d, J=4.7 Hz, 2 H), 3.85 (dd, J=10.7, 3.6 Hz, 1 H), 3.74 (dd, J=10.7, 6.2 Hz, 1 H), 2.41 (s, 3 H, Ts CH₃), 1.43, 1.19 (2 x s, 2 x 3 H, *i*-propylidene CH₃). ¹³C NMR (100 MHz, CDCl₃) δ (ppm) 158.6 (1 C, C-6), 151.5, 149.7, 145.6, 144.5, 132.3 (7 C, C-2, C-4, Ts C-1, Ts C-4, 3 x Trt arom C_q), 130.1, 128.9, 127.9, 127.9, 127.1 (19 C, arom.), 118.4 (1 C, C-5), 114.3 (1 C, *i*-propylidene C_q), 90.7 (1 C, C-1'), 83.3, 82.3, 80.9 (3 C, C-2', C-3', C-4'), 71.3 (1 C, N-TrtC_q), 68.9 (1 C, C-6'), 27.3, 25.9 (2 C, 2 x *i*-propylidene CH₃), 21.8 (1 C, Ts CH₃). MALDI ToF MS: m/z calcd for C₃₉H₃₇N₅NaO₇S [M+Na]⁺ 742.231, found 742.241.

2',3'-O-Isopropylidene-O, N-ditrityl-cytidine (15): 2',3'-O-Isopropylidene-cytidine **14** (0.927 g, 3.27 mmol) was dissolved in dry pyridine (10 mL). TrtCl (3.7 g, 13.08 mmol, 4.0 equiv.) was added and the reaction mixture was stirred at 60 °C for 3 days. Since the conversion was not complete, another portion of TrtCl (462 mg, 0.5 equiv.) and DMAP (20 mg, 0.05 equiv) was added and the solution was stirred at 60 °C for 4 days. The solvent was evaporated *in vacuo*. The crude product was purified by flash column chromatography (gradient elution CH₂Cl₂ → CH₂Cl₂:MeOH 98:2) to give **15** (1.30 g, 39%) as a white solid. [α]_D²⁰ = -8.75 (c=0.40, CHCl₃), Rf=0.63 (CH₂Cl₂/MeOH 98/2), ¹H NMR (400 MHz, CDCl₃) δ (ppm) 8.58 (d, J=4.2 Hz, 1 H, NH), 7.35–7.09 (m, 31 H, arom.), 6.89 (s, 1 H, H-6), 5.90 (d, J=1.6 Hz, 1 H, H-1'), 4.87 (dd, J=6.2, 1.7 Hz, 1 H, H-2'), 4.77 (d, J=3.4 Hz, 1 H, H-5), 4.75 (d, J=4.5 Hz, 1 H, H-3'), 4.29 (dd, J=7.0, 4.1 Hz, 1 H, H-4'), 3.44 (dd, J=10.7, 4.6 Hz, 1 H), 3.36 (dd, J=10.7, 2.4 Hz, 1 H), 1.53, 1.32 (2 x s, 2 x 3 H, 2 x *i*-propylidene CH₃). ¹³C NMR (100 MHz, CDCl₃) δ (ppm) 165.65 (1 C, C-4), 155.00 (1 C, C-2), 143.92, 143.24 (6 C, arom. C_q), 141.90 (1 C, C-6), 128.69, 128.66, 128.36, 127.90, 127.57, 127.21 (30 C, arom.), 113.78 (1 C, *i*-propylidene C_q), 87.27 (1 C, O-Trt C_q), 94.47, 93.36, 86.43, 85.76, 80.50 (5 C, C-1', C-2', C-3', C-4', C-5), 70.85 (1 C, N-Trt C_q), 63.78 (1 C, C-5'), 27.32, 25.48 (2 C, 2 x *i*-propylidene CH₃). MALDI-ToF MS: m/z calcd for C₅₀H₄₅N₃NaO₅ [M+Na]⁺ 790.33, found 790.43.

2',3'-O-Isopropylidene-N-trityl-cytidine (16): Compound **15** (500 mg, 0.651 mmol) was added to the mixture of HFIP (6.5 mL), Et₃SiH (395 μL, 2.47 mmol, 3.8 equiv.) and BF₃·Et₂O (10.4 μL, 0.0846 mmol, 0.13 equiv). When the yellow colour of the solution was disappeared the reaction was monitored by TLC (hexane/acetone 65/35 R_f=0.19). After complete conversion of the starting compound (1 h) the reaction was quenched by saturated aq. solution of NaHCO₃ (0.5 mL). The solvent was evaporated *in vacuo* and the residue was purified by flash column chromatography (gradient elution hexane: acetone 65:35 → 6:4 → 1:1) to give **16** (315 mg = 92%) as a white solid. [α]_D²⁰ = -46.0 (c=0.25, CHCl₃), Rf=0.19 (hexane/acetone 65/35), ¹H NMR (400 MHz, CDCl₃) δ (ppm) 7.41–7.15 (m, 15 H, arom.), 7.02 (d, J=7.5 Hz, 1 H, H-6), 5.09 (d, J=2.7 Hz, 1 H, H-1'), 5.05 (d, J=7.5 Hz, 1 H, H-5), 4.38 (s, 0.5 H), 4.27 (d, J=2.2 Hz, 1 H), 3.88 (d, J=12.2 Hz, 1 H), 3.75 (d, J=10.6 Hz, 1 H), 1.52, 1.33 (2 x s, 2 x 3 H, 2 x *i*-propylidene CH₃). ¹³C NMR (100 MHz, CDCl₃) δ (ppm) 166.02 (1 C, C-4), 155.22 (1 C, C-2), 144.73 (1 C, C-6), 143.68 (3 C, arom C_q), 128.67, 128.50, 127.75 (15 C, arom.), 113.84 (1 C, *i*-propylidene C_q), 99.07, 94.98, 87.81, 83.32, 80.54 (C-1', C-2', C-3', C-4', C-5), 71.07 (1 C, N-TrtC_q), 62.83 (1 C, C-5'), 27.27, 25.24 (2 C, 2 x *i*-propylidene CH₃). MALDI-ToF MS: m/z calcd for C₃₁H₃₁N₃NaO₅ [M+Na]⁺ 548.22, found 548.38.

2',3'-O-Isopropylidene-5'-O-tosyl-N-trityl-cytidine (17): Compound **16** (1.86 g, 3.5 mmol) was dissolved in dry pyridine (10 mL) and TsCl (1.33 g, 7.0 mmol, 2.0 equiv.) was added and stirred overnight. Next day, water was added to the reaction mixture and stirred for an hour. The solvent was evaporated under reduced pressure and the residue was dissolved in CH₂Cl₂ (300 mL). The organic phase was extracted with satd. aq. NaHCO₃, 10% aq. NaHSO₄ and water, then dried over Na₂SO₄, filtered and evaporated *in vacuo*. The crude product was purified by flash chromatography (hexane: acetone 75:25) to give **17** (303 mg, 13%) as a white foam. [α]_D²⁰ = +37.7 (c=0.13, CHCl₃), Rf=0.37 (hexane/acetone 6/4), ¹H NMR (400 MHz, CDCl₃) δ (ppm) 7.75 (d, J=8.3 Hz, 1 H), 7.56 (d, J=8.1 Hz, 1 H), 7.38–7.14 (m, 23 H), 7.02 (d, J=8.0 Hz, 1 H), 6.92 (d, J=7.6 Hz, 1 H), 5.35 (s, 1 H), 5.07 (s, 1 H), 5.00 (s, 1 H), 4.81 (d, J=6.4 Hz, 1 H), 4.77 (d, J=2.1 Hz, 1 H), 2.42 (s, 3 H, Ts CH₃), 1.48, 1.28 (2 x s, 2 x 3 H, 2 x *i*-propylidene CH₃). ¹³C NMR (100 MHz, CDCl₃) δ (ppm) 166.1 (1 C, C-4), 154.6 (1 C, C-2), 144.9 (1 C, C-6), 144.1, 143.8, 142.8, 132.9 (5 C, Ts C-1, Ts C-4, 3 x Trt arom C_q), 129.9, 129.1, 128.7, 128.5, 128.4, 128.0, 127.8, 127.0, 126.2 (19 C, arom.), 113.9 (1 C, *i*-propylidene C_q), 97.8, 94.8, 86.6, 84.7, 81.9 (5 C, C-1', C-2', C-3', C-4', C-5), 71.1, 70.3 (2 C, C-5', N-Trt C_q), 27.0, 25.2, 21.7 (3 C, Ts CH₃, *i*-propylidene CH₃). MALDI-ToF MS: m/z calcd for C₃₈H₃₇N₃NaO₅S [M+Na]⁺ 702.22, found 702.40.

5'-Bromo-5'-deoxy-2',3'-O-isopropylidene-uridine (20)⁵¹: Compound **5** (6.6 g, 15.1 mmol), and Bu₄NBr (6.3 g 19.6 mmol, 1.3 equiv.) were dissolved in acetone (50 mL) and stirred for 2.5 h at 80 °C. The solvent was evaporated under reduced pressure. The crude product was purified by flash column chromatography (hexane: acetone 7:3) to give **20** (5 g, 94%) as white foam. [α]_D²⁰ = +12.92 (c=0.48, CHCl₃), Rf=0.22 (hexane/acetone 7/3), ¹H NMR (400 MHz, CDCl₃) δ (ppm) 10.13 (s, 1 H, NH), 7.37 (d, J=8.0 Hz, 1 H, H-6), 5.78 (dd, J=8.0, 1.2 Hz,

1 H, H-5), 5.67 (d, $J=2.1$ Hz, 1 H, H-1'), 5.04 (dd, $J=6.5, 2.1$ Hz, 1 H, H-2'), 4.90 (dd, $J=6.5, 3.7$ Hz, 1 H, H-3'), 4.38 (td, $J=5.8, 3.8$ Hz, 1 H, H-4'), 3.69 (dd, $J=10.6, 6.4$ Hz, 1 H, H-5'a), 3.57 (dd, $J=10.6, 5.4$ Hz, 1 H, H-5'b), 1.58 (s, 3 H, *i*-propylideneCH₃), 1.37 (s, 3 H, *i*-propylideneCH₃). ¹³C NMR (100 MHz, CDCl₃) δ (ppm) 164.0, 150.2 (2 C, C-2, C-4), 142.9 (1 C, C-6), 114.8 (1 C, *i*-propylideneC_q), 102.9 (1 C, C-5), 95.3 (1 C, C-1'), 86.8, 84.5, 83.2 (3 C, C-2', C-3', C-4'), 32.4 (1 C, C-5'), 27.1, 25.3 (2 C, 2x *i*-propylideneCH₃). MALDI ToF MS: m/z calcd for C₁₂H₁₅BrN₂NaO₅ [M + Na]⁺ 369.006, found 369.010.

S-(2',3'-O-Isopropylidene-uridine-5'-yl)-dithioacetic acid (21): Method A: CS₂ (91 μ L, mmol, 3.0 equiv.) was dissolved in dry THF (4 mL) under Ar and MeMgBr 3 M solution in diethyl ether (0.5 mL, 1.5 mmol, 3.0 equiv.) was added and stirred overnight. Next day, compound 5 (219 mg, 0.5 mmol) was added and stirred at 80 °C for 5 h. The solvent was evaporated under reduced pressure and the crude product was purified by flash chromatography (hexane: acetone 85:15 \rightarrow 7:3) to give 152 mg of the unseparable mixture of 20 and 21 with approximately 1.4:1 ratio, as a yellow foam. **Method B:** CS₂ (1.0 mL, 17.1 mmol, 3.0 equiv.) was dissolved in dry THF (46 mL) under Ar and MeMgBr (3 M solution, in diethyl ether, 5.7 mL, 17.1 mmol, 3.0 equiv.) was added and stirred overnight. Next day, compound 5 (2.5 g, 5.7 mmol) was added and stirred at 80 °C for 18 h. The solvent was evaporated under reduced pressure and the crude product was purified by flash chromatography (hexane: acetone 85:15 \rightarrow 7:3) to give 21 (1.63 g, 80%) as a yellow foam. $[\alpha]_D^{25} = +33.0$ (c=0.20, CHCl₃), Rf=0.28 (hexane/acetone 7/3), ¹H NMR (400 MHz, CDCl₃) δ (ppm) 9.92 (s, 1 H, NH), 7.23 (d, $J=8.0$ Hz, 1 H, H-6), 5.76 (d, $J=8.0$ Hz, 1 H, H-5), 5.53 (d, $J=1.4$ Hz, 1 H, H-1'), 5.09 (dd, $J=6.5, 1.6$ Hz, 1 H, H-2'), 4.82 (dd, $J=6.4, 4.1$ Hz, 1 H, H-3'), 4.32 (td, $J=6.6, 4.2$ Hz, 1 H, H-4'), 3.72–3.60 (m, 2 H, H-5'ab), 2.86 (s, 3 H, thioAc CH₃), 1.54 (s, 3 H, *i*-propylidene CH₃), 1.35 (s, 3 H, *i*-propylidene CH₃). ¹³C NMR (100 MHz, CDCl₃) δ (ppm) 232.1 (1 C, CS), 163.8, 150.2 (2 C, C-2, C-4), 143.3 (1 C, C-6), 114.7 (1 C, *i*-propylidene C_q), 102.8 (1 C, C-5), 96.1 (1 C, C-1'), 85.6, 84.7, 83.8 (3 C, C-2', C-3', C-4'), 39.4 (1 C, thioAc CH₃), 39.1 (1 C, C-5'), 27.2, 25.3 (2 C, 2x *i*-propylidene CH₃). MALDI ToF MS: m/z calcd for C₁₄H₁₈N₂NaO₅S₂ [M + Na]⁺ 381.055, found 381.065.

S-(Uridine-5'-yl)-dithioacetic acid (22): Compound 21 (2.64 g, 7.36 mmol) was dissolved in 90% aq. TFA (20 mL) and stirred for 2 h at r.t. The solvent was evaporated under reduced pressure, and co-evaporated with toluene. The crude product was purified by flash column chromatography (CH₂Cl₂:MeOH 97.5:2.5 \rightarrow 96:4 \rightarrow 95:5) to give 22 (1.3 g, 57%) as yellow solid. $[\alpha]_D^{25} = +22.0$ (c=0.10, DMSO), Rf=0.60 (CH₂Cl₂/MeOH 9/1), ¹H NMR (400 MHz, MeOD) δ (ppm) 7.60 (d, $J=8.1$ Hz, 1 H, H-6), 5.79 (d, $J=4.8$ Hz, 1 H, H-1'), 5.74 (d, $J=8.1$ Hz, 1 H, H-5), 4.28 (t, $J=5.2$ Hz, 1 H, H-2'), 4.15–4.08 (m, 1 H, H-4'), 4.03 (t, $J=5.3$ Hz, 1 H, H-3'), 3.76 (dd, $J=13.9, 5.1$ Hz, 1 H, H-5'a), 3.61 (dd, $J=13.9, 7.4$ Hz, 1 H, H-5'b), 2.85 (s, 3 H, CH₃). ¹³C NMR (100 MHz, MeOD) δ (ppm) 234.2 (1 C, CS), 166.0, 152.2 (2 C, C-2, C-4), 142.8 (1 C, C-6), 103.1 (1 C, C-5), 91.9 (1 C, C-1'), 82.7 (1 C, C-4'), 74.5 (1 C, C-1'), 74.1 (1 C, C-3'), 40.2 (1 C, C-5'), 39.5 (1 C, CH₃). MALDI ToF MS: m/z calcd for C₁₁H₁₄N₂NaO₅S₂ [M + Na]⁺ 341.0236, found 341.0231.

S-(2',3'-O-Isopropylidene-N-trityl-adenosine-5'-yl)-dithioacetic acid (23): Method A: CS₂ (257 μ L, 4.26 mmol, 3.0 equiv.) was dissolved in dry THF (10 mL) under Ar and MeMgBr 3 M solution in diethyl ether (1.42 mL, 4.26 mmol, 3.0 equiv.) was added and stirred overnight. Next day, compound 9 (1.0 g, 1.42 mmol) was added and stirred at 80 °C for 18 h. The solvent was evaporated under reduced pressure and the crude product was purified by flash chromatography (hexane: acetone 9:1 \rightarrow 8:2) to give 23 (251 mg, 72%) as a yellow foam. **Method B:** Compound 9 (100 mg, 0.142 mmol) was dissolved in acetone (5 mL) and potassium-dithioacetate (37 mg, 0.284 mmol, 2.0 equiv.) was added and stirred at r.t. overnight. The solvent was evaporated and the residue was dissolved in CH₂Cl₂ (150 mL) and extracted with H₂O (3 \times 50 mL). The organic phase was dried over Na₂SO₄, filtered and evaporated under reduced pressure. The crude product was purified by flash chromatography (hexane/acetone 85/15) to give 23 (64 mg, 72%) as a yellow foam. $[\alpha]_D^{25} = +15.8$ (c=0.12, DMSO), Rf=0.25 (hexane/acetone 8/2), ¹H NMR (400 MHz, CDCl₃) δ (ppm) 8.03, 7.83 (2x s, 2 \times 1 H, H-2, H-8), 7.34 (d, $J=7.0$ Hz, 6 H, arom.), 7.30–7.20 (m, 9 H, arom.), 6.98 (s, 1 H, NH), 6.02 (s, 1 H, H-1'), 5.51 (d, $J=7.6$ Hz, 1 H, H-2'), 5.00 (dd, $J=6.2, 3.1$ Hz, 1 H, H-3'), 4.43 (dt, $J=6.8, 3.2$ Hz, 1 H, H-4'), 3.68 (dd, $J=13.8, 6.6$ Hz, 1 H, H-5'a), 3.58 (dd, $J=13.8, 7.2$ Hz, 1 H, H-5'b), 2.81 (s, 3 H, thioAc CH₃), 1.57 (s, 3 H, *i*-propylidene CH₃), 1.36 (s, 3 H, *i*-propylidene CH₃). ¹³C NMR (100 MHz, CDCl₃) δ (ppm) 231.9 (1 C, CS), 154.4, 148.2, 121.7 (3 C, C-4, C-5, -6), 152.5 (1 C, adenine CH), 145.0 (3 C, 3x Trt arom C_q), 129.1, 128.0, 127.1 (15 C, arom.), 114.7 (1 C, *i*-propylidene C_q), 91.1 (1 C, C-1'), 84.8, 84.23, 84.1 (3 C, C-2', C-3', C-4'), 39.3 (1 C, thioAc CH₃), 39.2 (1 C, C-5'), 27.2, 25.4 (2 C, 2x *i*-propylidene CH₃). MALDI ToF MS: m/z calcd for C₃₄H₃₃N₅NaO₃S₂ [M + Na]⁺ 646.192, found 646.204.

S-(Adenosine-5'-yl)-dithioacetic acid (24): Compound 23 (218 mg, 0.35 mmol) was dissolved in 90% aq. TFA (5 mL) Et₃SiH (167 μ L, 1.05 mmol, 3.0 equiv.) was added and stirred for 2 h at r.t. The solvent was evaporated under reduced pressure, and co-evaporated with toluene. The crude product was purified by flash column chromatography (CH₂Cl₂:MeOH 98:2 \rightarrow 97:3 \rightarrow 95:5) to give 24 (76 mg, 64%) as yellow solid. $[\alpha]_D^{25} = -7.14$ (c=0.14, DMSO), Rf=0.1 (CH₂Cl₂/MeOH 95/5), ¹H NMR (400 MHz, MeOD) δ (ppm) 8.23, 8.20 (2x s, 2 \times 1 H, H-2, H-8), 5.97 (d, $J=5.3$ Hz, 1 H, H-1'), 4.92 (t, $J=5.3$ Hz, 1 H, H-2'), 4.31 (d, $J=4.3$ Hz, 1 H, H-3'), 4.28–4.21 (m, 1 H, H-4'), 3.83 (dd, $J=13.9, 5.5$ Hz, 1 H, H-5'a), 3.72 (dd, $J=13.9, 7.3$ Hz, 1 H, H-5'b), 2.82 (s, 3 H, thioAc CH₃). ¹³C NMR (100 MHz, MeOD) δ (ppm) 234.3 (1 C, CS), 153.9 (1 C, adenine CH), 90.4 (1 C, C-1'), 83.5 (1 C, C-4'), 74.6 (2 C, C-3', C-2'), 40.4 (1 C, C-5'), 39.4 (1 C, thioAc CH₃). MALDI ToF MS: m/z calcd for C₁₂H₁₆N₅O₃S₂ [M + H]⁺ 342.0689, found 342.0689.

5'-Bromo-5'-deoxy-2',3'-O-isopropylidene-N-trityl-guanosine (25): CS₂ (126 μ L, 2.08 mmol, 3.0 equiv.) was dissolved in dry THF (5 mL) under Ar and MeMgBr 3 M solution in diethyl ether (126 μ L, 2.08 mmol, 3.0 equiv.) was added and stirred overnight. Next day, compound 13 (500 mg, 0.6976 mmol) was added and stirred at 80 °C for 24 h. The solvent was evaporated under reduced pressure and the crude product was purified by flash chromatography (CH₂Cl₂:MeOH 98:2 \rightarrow 97:3 \rightarrow 96:4 \rightarrow 95:5) to give 25 (335 mg, 77%) as a yellowish solid. $[\alpha]_D^{25} = +39.1$ (c=0.32, CHCl₃), Rf=0.3 (CH₂Cl₂/MeOH 9/1), ¹H NMR (400 MHz, CDCl₃) δ (ppm) 11.69 (s, 1 H, NH), 7.85 (s, 1 H), 7.31 (t, $J=7.7$ Hz, 8 H, arom.), 7.16 (dt, $J=24.6, 7.4$ Hz, 12 H, arom.), 7.04 (s, 1 H, arom.), 5.33

(d, $J = 3.4$ Hz, 1 H, H-1'), 4.59 (dd, $J = 5.9, 3.5$ Hz, 1 H), 4.19–4.10 (m, 2 H), 2.94 (dd, $J = 10.6, 5.9$ Hz, 1 H, H-5'a), 2.82 (dd, $J = 10.5, 7.6$ Hz, 1 H, H-5'b), 1.46 (s, 3 H, *i*-propylidene CH_3), 1.23 (s, 3 H, *i*-propylidene CH_3). ^{13}C NMR (100 MHz, $CDCl_3$) δ (ppm) 158.8, 151.4, 149.7, 118.6 (4 C, C-2, C-4', C-5, C-6), 144.5 (3 C, 3 x Trt arom C_q), 128.9, 127.8, 126.9 (15 C, arom.), 114.2 (1 C, *i*-propylidene C_q), 90.9, 84.3, 82.6, 81.3 (4 C, C-1', C-2', C-3', C-4'), 71.0 (1 C, Trt C_q), 31.5 (1 C, C-5'), 27.4, 25.9 (2 C, 2 x *i*-propylidene CH_3). MALDI ToF MS: m/z calcd for $C_{32}H_{30}BrN_5NaO_4 [M + Na]^+$ 650.137, found 650.147.

S-(2',3'-O-Isopropylidene-*N*-trityl-guanosine-5'-yl)-dithioacetic acid (26): CS_2 (173 μ L, 2.86 mmol, 6.0 equiv.) was dissolved in dry THF (6 mL) under Ar and MeMgBr (3 M solution in diethyl ether, 0.95 mL, 2.86 mmol, 6.0 equiv.) was added and stirred overnight. Next day, compound **25** (300 mg, 0.477 mmol) was added and stirred at 80 °C for 28 h. The solvent was evaporated under reduced pressure and the crude product was purified by flash chromatography (CH_2Cl_2 :MeOH 95:5) to give **26** (259 mg, 85%) as a yellow solid. $[\alpha]_D = +39.1$ ($c = 0.32$, $CHCl_3$), $R_f = 0.3$ (CH_2Cl_2 /MeOH 9/1), 1H NMR (400 MHz, DMSO) δ (ppm) 10.79 (s, 1 H, NH), 7.76 (s, 1 H), 7.72 (s, 1 H), 7.36–7.22 (m, 15 H, arom.), 5.51 (d, $J = 3.3$ Hz, 1 H, H-1'), 4.76 (d, $J = 5.7$ Hz, 1 H), 4.06 (s, 1 H), 4.01 (t, $J = 7.2$ Hz, 1 H), 3.14 (dd, $J = 13.9, 6.3$ Hz, 1 H, H-5'b), 2.99 (dd, $J = 13.7, 8.3$ Hz, 1 H, H-5'a), 2.79 (d, $J = 13.6$ Hz, 3 H, thioAc CH_3), 1.36 (s, 3 H, *i*-propylidene CH_3), 1.20 (s, 3 H, *i*-propylidene CH_3). ^{13}C NMR (100 MHz, DMSO) δ (ppm) 156.3, 151.2, 148.9, 118.1 (4 C, C-2, C-4, C-5, C-6), 144.5 (3 C, 3 x Trt arom C_q), 128.4, 127.9, 126.9 (15 C, arom.), 113.4 (1 C, *i*-propylidene C_q), 89.3, 82.8, 81.1, 80.6 (4 C, C-1', C-2', C-3', C-4'), 70.3 (1 C, Trt C_q), 39.2 (1 C, thioAc CH_3), 39.1 (1 C, C-5'), 27.0, 25.7 (2 C, 2 x *i*-propylidene CH_3). MALDI ToF MS: m/z calcd for $C_{34}H_{33}N_5NaO_4S_2 [M + Na]^+$ 662.1866, found 662.1876.

S-(Guanosine-5'-yl)-dithioacetic acid (27): Compound **26** (221 mg, 0.35 mmol) was dissolved in 90% aq. TFA (5 mL), Et_3SiH (167 μ L, 1.05 mmol, 3.0 equiv.) was added and stirred for 2 h at r.t. The solvent was evaporated under reduced pressure. The crude product was purified by flash column chromatography (CH_2Cl_2 :MeOH 9:1→85:15→8:2) to give **27** (89 mg, 72%) as yellow solid. $[\alpha]_D = -5.45$ ($c = 0.11$, DMSO), $R_f = 0.44$ (CH_2Cl_2 /MeOH 8/2), 1H NMR (400 MHz, DMSO) δ (ppm) 10.80 (s, 1 H, NH), 7.90 (s, 1 H), 6.61 (s, 2 H), 5.68 (d, $J = 6.0$ Hz, 1 H, H-1'), 5.57 (d, $J = 6.1$ Hz, 1 H, 2'-OH), 5.40 (d, $J = 4.9$ Hz, 1 H, 3'-OH), 4.64 (dd, $J = 11.3, 5.8$ Hz, 1 H, H-2'), 4.10–4.05 (m, 1 H, H-3'), 4.02–3.97 (m, 1 H, H-4'), 3.71 (dd, $J = 13.7, 5.5$ Hz, 1 H, H-5'a), 3.59 (dd, $J = 13.7, 8.0$ Hz, 1 H, H-5'b), 2.83 (s, 3 H, thioAc CH_3). ^{13}C NMR (100 MHz, DMSO) δ (ppm) 233.9 (1 C, CS), 156.8, 153.8, 151.4, 116.9 (4 C, C-2, C-4, C-5, C-6), 136.63*, 86.8 (1 C, C-1'), 81.2 (1 C, C-4'), 72.9, 72.6 (2 C, C-2', C-3'). * Can only be seen in HSQC. MALDI ToF MS: m/z calcd for $C_{12}H_{15}N_5NaO_4S_2 [M + Na]^+$ 380.0458, found 380.0454.

S-(2',3'-O-Isopropylidene-*N*-trityl-cytidine-5'-yl)-dithioacetic acid (28): CS_2 (692 μ L, 11.4 mmol, 6.0 equiv.) was dissolved in dry THF (24 mL) under Ar and MeMgBr (3 M solution in diethyl ether, 3.82 mL, 11.4 mmol, 6.0 equiv.) was added and stirred overnight. Next day, compound **17** (1.3 mg, 1.91 mmol) was added and stirred at 80 °C for 18 h. The solvent was evaporated under reduced pressure and the crude product was purified by flash chromatography (CH_2Cl_2 :MeOH 100:0.5→100:1→100:2) to give **28** (1 g, 95%) as a yellow solid. $[\alpha]_D = +37.5$ ($c = 0.16$, $CHCl_3$), $R_f = 0.3$ (hexane/acetone 6/4), 1H NMR (400 MHz, $CDCl_3$) δ (ppm) 7.37–7.27 (m, 10 H, arom.), 7.26–7.20 (m, 7 H, arom.), 6.91 (6.92 (d, $J = 7.6$ Hz, 1 H, H-6), 5.27 (s, 1 H, H-1'), 5.25 (s, 1 H, H-2'), 5.01 (d, $J = 7.5$ Hz, 1 H, H-5), 4.93 (dd, $J = 6.3, 3.5$ Hz, 1 H, H-3'), 4.30 (td, $J = 6.8, 3.6$ Hz, 1 H, H-4'), 3.82–3.77 (m, 1 H, H-5'a), 3.72 (dd, $J = 13.7, 7.3$ Hz, 1 H, H-5'b), 2.83 (s, 3 H, thioAc CH_3), 1.49 (s, 3 H, *i*-propylidene CH_3), 1.32 (s, 3 H, *i*-propylidene CH_3). ^{13}C NMR (100 MHz, $CDCl_3$) δ (ppm) 232.3 (1 C, CS), 166.1, 154.6 (2 C, C-2, C-4), 144.5 (1 C, C-6), 143.8 (3 C, 3 x Trt arom C_q), 128.7, 128.5, 127.7 (15 C, arom.), 113.7 (1 C, *i*-propylidene C_q), 98.6 (1 C, C-1'), 94.7 (1 C, C-5), 86.6 (1 C, C-4'), 84.9, 84.6 (2 C, C-2', C-3'), 71.1 (1 C, Trt C_q), 39.3, 39.2 (1 C, thioAc CH_3), 29.3 (1 C, C-5'), 26.9, 25.1 (2 C, 2 x *i*-propylidene CH_3). MALDI ToF MS: m/z calcd for $C_{33}H_{33}N_3NaO_4S_2 [M + Na]^+$ 622.181, found 622.154.

S-(Cytidine-5'-yl)-dithioacetic acid (29): Compound **28** (1 g, 1.69 mmol) was dissolved in 90% aq. TFA (10 mL), Et_3SiH (808 μ L, 5.07 mmol, 3.0 equiv.) was added and stirred for 2 h at r.t. The solvent was evaporated under reduced pressure, and co-evaporated with toluene. The crude product was purified by flash column chromatography (CH_2Cl_2 :MeOH 9:1) to give **29** (379 mg, 73%) as yellow solid. $[\alpha]_D = +40.8$ ($c = 0.12$, $CHCl_3$), $R_f = 0.18$ (CH_2Cl_2 /MeOH 9/1), 1H NMR (400 MHz, MeOD) δ (ppm) 7.76 (d, $J = 7.7$ Hz, 1 H, H-6), 6.06 (d, $J = 7.6$ Hz, 1 H, H-5), 5.80 (d, $J = 3.9$ Hz, 1 H, H-1'), 4.27 (d, $J = 4.6$ Hz, 1 H, H-2'), 4.15 (dd, $J = 12.7, 5.4$ Hz, 1 H, H-4'), 4.01 (t, $J = 5.6$ Hz, 1 H, H-3'), 3.80 (dd, $J = 13.9, 4.9$ Hz, 1 H, H-5'a), 3.63 (dd, $J = 13.9, 7.6$ Hz, 1 H, H-5'b), 2.86 (s, 3 H, thioAc CH_3). ^{13}C NMR (100 MHz, MeOD) δ (ppm) 234.2 (1 C, CS), 165.1 (2 C, C-2, C-4), 144.3 (1 C, C-6), 96.3, 92.9 (2 C, C-1', C-5), 82.8 (1 C, C-4), 75.2, 74.1 (2 C, C-2', C-3'), 40.2 (1 C, C-5'), 39.4 (1 C, thioAc CH_3). MALDI ToF MS: m/z calcd for $C_{11}H_{15}N_3NaO_4S_2 [M + Na]^+$ 340.0396, found 340.0404.

S-(Thymidine-5'-yl)-dithioacetic acid (30): CS_2 (457 μ L, 7.6 mmol, 3.0 equiv.) was dissolved in dry THF (15 mL) under Ar and MeMgBr 3 M solution in diethyl ether (2.53 mL, 7.57 mmol, 3.0 equiv.) was added and stirred overnight. Next day, compound **18** (1.0 g, 2.52 mmol) was added and stirred at 80 °C for 18 h. The solvent was evaporated under reduced pressure and the crude product was purified by flash chromatography (CH_2Cl_2 :MeOH 96:4→95:5) to give **30** (568 mg, 72%) as a yellow solid. $[\alpha]_D = +42.7$ ($c = 0.36$, DMSO), $R_f = 0.44$ (CH_2Cl_2 /MeOH 95/5), 1H NMR (400 MHz, DMSO) δ (ppm) 11.32 (s, 1 H, NH), 7.46 (s, 1 H, H-6), 6.17 (t, $J = 6.9$ Hz, 1 H, H-1'), 5.46 (s, 1 H, OH), 4.19 (s, 1 H, H-3'), 3.89 (s, 1 H, H-4'), 3.66 (dd, $J = 13.6, 5.3$ Hz, 1 H, H-5'a), 3.53 (dd, $J = 13.5, 7.8$ Hz, 1 H, H-5'b), 2.85 (s, 3 H, thioAc CH_3), 2.29 (dt, $J = 13.7, 6.9$ Hz, 1 H, H-2'a), 2.15–2.05 (m, 1 H, H-2'b), 1.81 (s, 3 H, thymine CH_3). ^{13}C NMR (100 MHz, DMSO) δ (ppm) 233.9 (1 C, CS), 163.9, 150.7 (2 C, C-2, C-4), 136.3 (1 C, C-6), 110.1 (1 C, C-5), 84.2 (1 C, C-1'), 83.2 (1 C, C-4'), 73.1 (1 C, C-3'), 39.6 (1 C, thioAc CH_3), 38.2 (1 C, C-2'), 12.3 (1 C, thymine CH_3). MALDI ToF MS: m/z calcd for $C_{12}H_{16}N_2NaO_4S_2 [M + Na]^+$ 339.0444, found 339.0438.

5'-S-Acetyl-5'-thiouridine (31): PPh₃ (6.5 g, 24.6 mmol, 2.0 equiv.) was dissolved in dry THF (50 mL) and cooled to 0 °C. DIAD (5.0 mL, 24.6 mmol, 2.0 equiv.) was added dropwise and stirred for 30 min at 0 °C. Uridine (3.0 g, 12.3 mmol) and HSAc (1.8 mL, 24.6 mmol, 2.0 equiv.) were dissolved in dry DMF (50 mL) and added dropwisely to the reaction mixture and stirred for 30 min at 0 °C and 30 min at r.t. The solvent was evaporated

under reduced pressure and the crude product was purified by flash column chromatography (gradient elution, CH_2Cl_2 :MeOH 97.5:2.5→9:1→8:2) to give **31** (2.5 g, 70%) as a pale yellowish solid. $[\alpha]_{\text{D}} = +17.8$ ($c = 0.23$, DMSO), $R_f = 0.16$ (CH_2Cl_2 /MeOH 95/5), $^1\text{H NMR}$ (400 MHz, DMSO) δ (ppm) 11.36 (s, 1 H, NH), 7.63 (d, $J = 8.1$ Hz, 1 H, H-6), 5.73 (d, $J = 5.6$ Hz, 1 H, H-1'), 5.67 (dd, $J = 8.0, 2.1$ Hz, 1 H, H-5), 5.43 (d, $J = 5.6$ Hz, 1 H, 2'-OH), 5.29 (d, $J = 4.5$ Hz, 1 H, 3'-OH), 4.14 (dd, $J = 10.2, 5.1$ Hz, 1 H, H-2'), 3.87–3.78 (m, 2 H, H-4', H-3'), 3.27 (dd, $J = 13.8, 5.0$ Hz, 1 H, H-5'a), 3.10 (dd, $J = 13.8, 7.0$ Hz, 1 H, H-5'b), 2.36 (s, 3 H, AcCH_3). $^{13}\text{C NMR}$ (100 MHz, DMSO) δ (ppm) 194.8 (1 C, AcCO), 163.1, 150.7 (2 C, C-2, C-4), 141.2 (1 C, C-6), 102.2 (1 C, C-5), 88.4, 82.3, 72.3, 72.2 (4 C, C-1', C-2', C-3', C-4'), 31.0 (1 C, C-5'), 30.5 (1 C, AcCH_3). MALDI-ToF MS: m/z calcd for $\text{C}_{11}\text{H}_{14}\text{N}_2\text{NaO}_6\text{S}$ $[\text{M} + \text{Na}]^+$ 325.0465, found 325.0423.

5'-Thiouridine (32)⁵²: Compound **31** (2.4 g, 8.0 mmol) was dissolved in dry MeOH (50 mL) under Ar, and NaOMe (648 mg, 12 mmol, 1.5 equiv.) was added and stirred at r.t. for 1 h. The reaction mixture was neutralized with Amberlite IR 120 H^+ ion exchanger resin, filtered off, and evaporated under reduced pressure. The crude product was purified by flash column chromatography (CH_2Cl_2 :MeOH 9:1) to give **32** (1.47 g, 71%) as a white solid. $[\alpha]_{\text{D}} = -40.8$ ($c = 0.13$, DMSO), $R_f = 0.24$ (CH_2Cl_2 /MeOH 95/5), $^1\text{H NMR}$ (400 MHz, DMSO) δ (ppm) 11.35 (s, 1 H, NH), 7.67 (d, $J = 8.1$ Hz, 1 H, H-6), 5.78 (d, $J = 6.0$ Hz, 1 H, H-1'), 5.67 (d, $J = 8.1$ Hz, 1 H, H-5), 5.41 (d, $J = 5.8$ Hz, 1 H, 2'-OH), 5.22 (d, $J = 5.0$ Hz, 1 H, 3'-OH), 4.13 (dd, $J = 11.3, 5.7$ Hz, 1 H, H-2'), 3.92 (dd, $J = 8.8, 4.6$ Hz, 1 H, H-3'), 3.85 (dd, $J = 9.5, 5.8$ Hz, 1 H, H-4'), 2.81 (dd, $J = 13.6, 5.5$ Hz, 1 H, H-5'a), 2.73 (dd, $J = 13.8, 6.0$ Hz, 1 H, H-5'b), 2.48 (d, $J = 19.6$ Hz, 1 H, SH). $^{13}\text{C NMR}$ (100 MHz, DMSO) δ (ppm) 172.6, 160.3 (2 C, C-2, C-4), 150.6 (1 C, C-6), 111.7 (1 C, C-5), 97.5, 94.1, 81.9, 81.0 (4 C, C-1', C-2', C-3', C-4'), 35.8 (1 C, C-5'). MALDI-ToF MS: m/z calcd for $\text{C}_9\text{H}_{12}\text{N}_2\text{NaO}_5\text{S}$ $[\text{M} + \text{Na}]^+$ 283.0359, found 283.0355.

5'-S-Acetyl-5'-thioadenosine (33): PPh_3 (6.5 g, 24.6 mmol, 2.0 equiv.) was dissolved in dry THF (50 mL) and cooled to 0 °C. DIAD (5.0 mL, 24.6 mmol, 2.0 equiv.) was added dropwise and stirred for 30 min at 0 °C. Adenosine (3.3 g, 12.3 mmol) and HSAc (1.8 mL, 24.6 mmol, 2.0 equiv.) were dissolved in dry DMF (50 mL) and added dropwise to the reaction mixture and stirred for 30 min at 0 °C and 90 min at r.t. The solvent was evaporated under reduced pressure and the crude product was purified by flash column chromatography (gradient elution, CH_2Cl_2 :MeOH 91→82) to give **33** (3.47 g, 87%) as a pale yellowish solid. $[\alpha]_{\text{D}} = -23.3$ ($c = 0.39$, DMSO), $R_f = 0.33$ (CH_2Cl_2 /MeOH 8/2), $^1\text{H NMR}$ (400 MHz, DMSO) δ (ppm) 8.35, 8.17 (2x s, 2×1 H, H-2, H-8), 7.33 (s, 2 H, NH_2), 5.89 (d, $J = 5.7$ Hz, 1 H, H-1'), 5.55 (d, $J = 6.1$ Hz, 1 H, 2'-OH), 5.41 (d, $J = 5.0$ Hz, 1 H, 3'-OH), 4.80 (dd, $J = 11.2, 5.7$ Hz, 1 H, H-2'), 4.12 (dd, $J = 8.9, 4.6$ Hz, 1 H, H-3'), 3.94 (dd, $J = 9.2, 7.2$ Hz, 1 H, H-4'), 3.36 (dd, $J = 13.8, 5.7$ Hz, 1 H, H-5'a), 3.18 (dd, $J = 13.5, 7.8$ Hz, 1 H, H-5'b), 2.33 (s, 3 H, AcCH_3). $^{13}\text{C NMR}$ (100 MHz, DMSO) δ (ppm) 195.3 (1 C, AcCO), 153.1 (2 C, C-2, C-8), 156.6, 149.9 (2 C, C-4, C-5), 119.7 (1 C, C-6), 88.0, 83.3, 73.1 (4 C, C-1', C-2', C-3', C-4'), 31.7 (1 C, C-5'), 30.9 (1 C, AcCH_3). MALDI-ToF MS: m/z calcd for $\text{C}_{12}\text{H}_{15}\text{N}_5\text{NaO}_4\text{S}$ $[\text{M} + \text{Na}]^+$ 348.074, found 348.067.

5'-Deoxy-5'-thioadenosine (34)⁵²: Compound **33** (3.16 g, 9.7 mmol) was dissolved in dry MeOH (50 mL) under Ar, and NaOMe (787 mg, 14.5 mmol, 1.5 equiv.) was added and stirred at r.t. for 1 h. The reaction mixture was neutralized with AcOH and evaporated under reduced pressure. The crude product was purified by flash column chromatography (CH_2Cl_2 :MeOH 9:1→8:2) to give **34** (2.11 g, 77%) as a white solid. $[\alpha]_{\text{D}} = -18.3$ ($c = 0.4$, DMSO), $R_f = 0.17$ (CH_2Cl_2 /MeOH 9/1), $^1\text{H NMR}$ (400 MHz, DMSO) δ (ppm) 8.37, 8.17 (2x s, 2×1 H, H-2, H-8), 7.32 (s, 2 H, NH_2), 5.91 (d, $J = 6.1$ Hz, 1 H, H-1'), 4.79 (t, $J = 5.6$ Hz, 1 H, H-2'), 4.25–4.19 (m, 1 H, H-3'), 3.99 (td, $J = 6.1, 3.3$ Hz, 1 H, H-4'), 2.89 (dd, $J = 13.7, 6.0$ Hz, 1 H, H-5'a), 2.78 (dd, $J = 13.8, 6.3$ Hz, 1 H, H-5'b) $^{13}\text{C NMR}$ (100 MHz, DMSO) δ (ppm) 156.1, 149.5 (2 C, C-4, C-5), 152.7 (2 C, C-2, C-8), 119.3 (1 C, C-6), 87.4, 85.5, 72.7, 71.9 (4 C, C-1', C-2', C-3', C-4'), 26.6 (1 C, C-5'). MALDI-ToF MS: m/z calcd for $\text{C}_{10}\text{H}_{14}\text{N}_5\text{O}_3\text{S}$ $[\text{M} + \text{H}]^+$ 284.0811, found 284.0804.

Detection of H_2S release of 5'-dithioacetyl nucleosides

The H_2S -donating ability of compound **22**, **24**, **27**, **29** and **30** (0.5 mg dissolved in 0.1 mL of DMSO) was detected in Dulbecco's modified Eagle's medium (DMEM) (4.9 mL) supplemented with 10% fetal bovine serum and 1% penicillin-streptomycin. The final concentrations were 0.31 mM for compound **22**, 0.29 mM for compound **24**, 0.28 mM for compound **27**, 0.32 mM for compound **29** and 0.32 mM for compound **30**, respectively. The released H_2S was detected by an amperometric, H_2S specific sensor (ISO-H2S-100, World Precision Instruments, Sarasota, FL, USA) connected to a WPI TBR 1025 One-Channel Free Radical Analyzer. The sensor was set to 10 nA range and poise voltage to +150 mV. Before the measurements the sensor was polarized in phosphate buffered saline (PBS) for 12 h¹⁹. The H_2S -release of NaHS was detected in distilled water (0.1 mg in 5 mL of H_2O ; 0.36 mM) and the H_2S -release of GYY4137 was measured in DMEM (0.5 mg of GYY4137 in 5 mL of medium; 0.27 mM).

Antioxidant assays

Determination of antioxidant activity by 2,2-diphenyl-1-picrylhydrazyl (DPPH) assay

DPPH is a stable free radical with a deep violet color that changes to yellow when neutralized by an electron or hydrogen radical, indicating the antioxidant activity of the sample being tested. The DPPH radical scavenging abilities were investigated following the method outlined by Shimamura et al., with minor adjustments⁵³. In this study, a cardiovascular tissue homogenate was used to induce H_2S release from the dithioacetate derivatives **22** and **24**, as well as GYY4137. A mixed solution of 1.2 mL of methanol and 800 μL of 0.1 M Tris-HCl buffer (pH 7.4) served as the blank. 1 mL DPPH solution was added to a mixture of methanol and 0.1 M Tris-HCl buffer (200:800 μL). After mixing, the absorbance was recorded at 517 nm on a UV-1600 PC VWR spectrophotometer (VWR, China). To avoid any potential interference from the heart extract in the assay, we measured the absorbance after adding different volumes of the extract into the mixture. These measurements were taken both immediately and after 30 min of incubation. Ultimately, the highest volume tested, 20 μL , which showed no activity at either time point, was selected for further tests.

The DPPH antioxidant assay was performed according to the following procedures. 1 mL of DPPH solution was added to a mixture of 200 μ L of the methanolic sample solution and 800 μ L of 0.1 M Tris-HCl buffer (pH = 7.4). For the groups containing the extract, the extract was introduced into a mixture of the sample solution in PBS buffer, 0.1 M Tris-HCl buffer, and DPPH (200:800:1000 μ L). Considering that GYY4137 produces H₂S upon hydrolysis, it was introduced last following the addition of the extract into a solution of PBS buffer, 0.1 M Tris-HCl buffer, and DPPH maintained at the same ratio. The same protocol was employed for NaHS without the addition of the extract. After mixing, the absorbance was promptly recorded, after which the solutions were incubated in the dark at room temperature for 30 min before the absorbance was measured again. The test samples were prepared and assayed at varying concentrations using a 2-fold serial dilution method, starting from a concentration of 2 mM. Each investigation was performed in triplicate, and the antioxidant activity was based on the absorbance recorded at 517 nm. Ascorbic acid (AA), GYY4137, and NaHS served as positive controls, while the unmodified nucleosides were used as reference compounds.

The inhibition ratio (IR) was calculated as follows:

$$\text{Inhibition Ratio (\%)} = \left(\frac{Ac - As}{Ac} \right) * 100$$

where *Ac* is the absorbance when methanol is added instead of the sample and *As* is the absorbance when the testing sample solution is added.

The antioxidant capacity was expressed as the concentration needed to achieve a 50% inhibition of the free radical (IC₅₀). The IC₅₀ values were calculated by plotting the percent of inhibition as a function of sample concentration.

ABTS decolorization assay

The ABTS decolorization assay was carried out as described by Szoke et al.⁵⁴ Briefly, the method is based on the scavenging of (2,2'-azinobis-(3-ethylbenzothiazoline-6-sulfonic acid) ABTS^{•+} radical cation. The decolorization caused by the compound is compared to the decolorization induced by Trolox (6-hydroxy-2,5,7,8-tetramethylchroman-2-carboxylic acid), and expressed as Trolox equivalent antioxidant capacity (TEAC) value. TEAC values were expressed as Trolox equivalents calculated from (Ai - Af)antioxidant/(Ai - Af) Trolox at 0.1 mM concentrations. Briefly, a total of 10 μ L sample, 20 μ L of Myoglobin Working Solution, and 150 μ L of ABTS Substrate Working Solution were mixed and incubated for 5 min at room temperature. At the end of incubation 100 mL of Stop Solution was added and endpoint absorbance at 405 nm was read. All experiments were performed in triplicates and repeated three times.

MTT assay

H9c2 viability was measured by MTT assay (3-(4,5-dimethylthiazol-2-yl)-2,5- (diphenyltetrazolium bromide)) on 96-well plates, according to the method described in the literature⁵⁵. Briefly, H9c2 cells were plated at density of (3 × 10³ cells/well) and grown overnight in a humidified incubator with 5% CO₂ at 37 °C for 24 h. For the determination of IC₅₀ values, cells were treated with the following conditions: fresh culture medium alone (control), fresh culture medium with compound **22**, **24**, **32** and **34** at concentrations ranging from 1 μ M to 1000 μ M for 24 h. After that, 20 μ L of 5 mg/mL MTT solution was added to each well. The plate was again incubated for 3 h at 37 °C. During incubation, a conversion of the water-soluble yellow dye MTT into an insoluble purple formazan by the action of mitochondrial reductase occurred. Formazan crystals were solubilized by adding 200 μ L of isopropanol to each well. The concentrations were determined by optical density at 570 nm. The background absorbance was also recorded at 690 nm, which was subtracted. Cell viability was expressed as a percent of the cell viability of the untreated control cells. After 24 h, cells were treated with compound **22**, **24**, **32** and **34**. On the next day, cell viability was measured by MTT assay as described previously⁵⁵.

Antiviral assay

Anti-SARS-CoV-2 activity and cytotoxicity determination in Calu-3 cells

The anti-SARS-CoV-2 activity was measured by determining the extent to which the compounds inhibited virus-induced cytopathic effect (CPE) in Calu-3 cells (ATCC). Briefly, 40,000 Calu-3 cells in a 96-well plate in DMEM medium with 2% FBS, 100 U of penicillin/mL and 100 μ g of streptomycin/mL (all Merck) were infected with SARS-CoV-2 (strain hCoV-19/Czech Republic/NRL_6632_2/2020) at multiplicity of infection 0.3. After 2 h, the medium was removed, cells were washed two times with 1X DMEM and two-fold serial dilutions of compounds from 1000 μ M were added in triplicate. Following two days incubation at 37 °C in 5% CO₂ the cell viability was determined by adding CellTiter-Glo luminescent cell reagent (Promega) using Tempest liquid dispenser (Formulatrix). The luminescent signal produced by ATP-dependent oxidation of luciferin by viable cells was measured using EnVision plate reader (Perkin Elmer). Drug concentrations required to reduce viral cytopathic effect by 50% (EC₅₀) were calculated using nonlinear regression from plots of percentage cell viability versus log₁₀ drug concentration using GraphPad Prism v.9.5.1 (GraphPad Software).

Cytotoxicity was evaluated by incubating the same two-fold serial dilutions of each compound with Calu-3 cells as above in the absence of the virus. Following two days incubation at 37 °C in 5% CO₂, the cell viability was determined as above. The compound concentrations resulting in 50% reduction of cell viability (CC₅₀) were calculated from plots of percentage of luminescence versus log₁₀ drug concentration as above. Remdesivir was used as control in both assays.

Virus yield reduction assay

The reduction in virus titer was assessed in medium after 2 days infection of Calu-3 in the Vero E6 cells by plaque assay. Briefly, 50 μ l of medium from Calu-3 cells infected in the presence of the highest compound concentration was mixed with DMEM medium followed by 10-fold dilution, mixed with Vero E6 cells, added to 24-well plate and incubated for 4 h at 37 °C in 5% CO₂. Next, the mixture was overlaid with 500 μ l of 3% carboxymethyl cellulose (Merck) and incubated for 5 days at 37 °C in 5% CO₂. Remdesivir was included as control. After incubation, the cells were washed once with 1 \times PBS, stained with naphthalene black (Merck), washed with water and air-dried. Plaques were counted and expressed as log₁₀ plaque forming units (PFU) per mL.

In vivo studies

The cardiac effects of adenosine, compound **22**, **24** and **34** were assessed with electrocardiography (ECG) and echocardiography on anaesthetized Sprague-Dawley rats (weighing 600–800 g, Charles River Laboratories) as described previously⁵⁶. The animals received humane care, and all experimental procedures were carried out in accordance with the “Principles of Laboratory Animal Care” by EU Directive 2010/63/EU. All experimental protocols were approved by the local Ethics Committee of University of Debrecen (25/2023/DEMÁB). Animal experiments are reported in compliance with the ARRIVE guidelines⁵⁷. Anesthesia was carried out using ketamine/xylazine mixture (100/10 mg/kg, i.m.). The chest was shaved and the animal was placed onto a heated pad (VisualSonics SR200, VisualSonics, Amsterdam, The Netherlands). The lateral tail vein was cannulated using a heparinized 26G i.v. cannula (BD Neoflon, BD Medical, NJ, USA). B-mode and M-mode echocardiography was carried out before and 30 s after the intravenous administration of the compounds. A high-resolution ultrasound machine (Vevo 3100 Imaging Station, VisualSonics, Amsterdam, The Netherlands) equipped with a 21 Hz transducer (MX201) was used for assessing cardiac parameters. Traces were obtained from the parasternal long axis view (PLAX). A B-mode video and an M-mode trace was recorded, and the following parameters were then offline analysed: left ventricle (LV) end-systolic and end-diastolic volume (LVESV, LVEDV, respectively) fractional shortening (FS) and ejection fraction (EF) and stroke volume (SV).

A 3-channel ECG was continuously recorded during the experiments (Vevo monitor ECG, VisualSonics, Amsterdam, The Netherlands). On the recorded ECG data, RR, PR and QT intervals, and heart rate (HR) were determined before and 30 s after the administration of the drugs, and 6 consecutive cardiac cycles were averaged for each parameter.

Statistical analyses for the in vivo studies were carried out using the GraphPad Prism 9.0 software (GraphPad Software, San Diego, CA, USA). Data distribution was assessed by the Shapiro-Wilk normality test, and paired t-test were used to determine the differences between the baseline (drug free) and endpoint (treated) parameters in each group. A multiple comparison was also carried out between the treatment groups by using one-way ANOVA with Tukey multiple comparison test. Data was shown as mean \pm SD, and differences with $p < 0.05$ were considered significant.

Data availability

The datasets used and/or analysed during the current study available from the corresponding author (A.B.) on reasonable request.

Received: 6 August 2024; Accepted: 2 January 2025

Published online: 22 January 2025

References

- Gadalla, M. M. & Snyder, S. H. Hydrogen sulfide as a gasotransmitter. *J. Neurochem.* **113**, 14–26. <https://doi.org/10.1111/j.1471-4159.2010.06580.x> (2010).
- Baskar, R. & Bian, J. Hydrogen sulfide gas has cell growth regulatory role. *Eur. J. Pharmacol.* **656**, 5–9. <https://doi.org/10.1016/j.ejphar.2011.01.052> (2011).
- Hellmich, M. R., Coletta, C., Chao, C. & Szabo, C. The therapeutic potential of cystathionine β -synthetase/hydrogen sulfide inhibition in cancer. *Antioxid. Redox Signal.* **22**, 424–448. <https://doi.org/10.1089/ars.2014.5933> (2015).
- Zaorska, E., Tomasova, L., Koszelewski, D., Ostaszewski, R. & Ufnal, M. Hydrogen sulfide in pharmacotherapy, beyond the hydrogen sulfide-donors. *Biomolecules* **10**, 323–348. <https://doi.org/10.3390/biom10020323> (2020).
- Aroca, A., Gotor, C., Bassham, D. C. & Romero, L. C. Hydrogen sulfide: from a toxic molecule to a key molecule of cell life. *Antioxidants* **9**, 621–644. <https://doi.org/10.3390/antiox9070621> (2020).
- Wallace, J. L. et al. A proof-of-concept, phase 2 clinical trial of the gastrointestinal safety of a hydrogen sulfide-releasing anti-inflammatory drug. *Br. J. Pharmacol.* **177**, 769–777. <https://doi.org/10.1111/bph.14641> (2020).
- Citi, V. et al. Searching for novel hydrogen sulfide donors: the vascular effects of two thiourea derivatives. *Pharmacol. Res.* **159**, 105039–105048. <https://doi.org/10.1016/j.phrs.2020.105039> (2020).
- Fu, L. et al. An antifungal role of hydrogen sulfide on the postharvest pathogens *Aspergillus Niger* and *Penicillium Italicum*. *PLoS One.* **9**, e104206. <https://doi.org/10.1371/journal.pone.0104206> (2014).
- Yang, G. H₂S as a potential defense against COVID-19? *Am. J. Physiol. Cell. Physiol.* **319**, C244–C249. <https://doi.org/10.1152/ajpcell.00187.2020> (2020).
- Evgenev, M. B. & Frenkel, A. Possible application of H₂S-producing compounds in therapy of coronavirus (COVID-19) infection and pneumonia. *Cell. Stress Chaperones.* **25**, 713–715. <https://doi.org/10.1007/s12192-020-01120-1> (2020).
- Dai, J., Teng, X., Jin, S. & Wu, Y. The antiviral roles of hydrogen sulfide by blocking the interaction between SARS-CoV-2 and its potential cell surface receptors. *Oxid. Med. Cell. Longev.* 2021 Article ID. **7866992** <https://doi.org/10.1155/2021/7866992> (2021).
- Bazhanov, N., Escaffre, O., Freiberg, A. N., Garofalo, R. P. & Casola, A. Broad-range antiviral activity of hydrogen sulfide against highly pathogenic RNA viruses. *Sci. Rep.* **7**, Article number 41029. <https://doi.org/10.1038/srep41029> (2017).
- Powell, C. R., Dillon, K. M. & Matson, J. B. A review of hydrogen sulfide (H₂S) donors: Chemistry and potential therapeutic applications. *Biochem. Pharmacol.* **149**, 110–123. <https://doi.org/10.1016/j.bcp.2017.11.014> (2018).
- Levin, C. M., Cerda, M. M. & Pluth, M. D. Activatable small-molecule hydrogen sulfide donors. *Antioxid. Redox Signal.* **32**, 96–109. <https://doi.org/10.1089/ars.2019.7841> (2020).

15. Kashfi, K. & Olson, K. R. Biology and therapeutic potential of hydrogen sulfide and hydrogen sulfide-releasing chimeras. *Biochem. Pharmacol.* **85**, 689–703. <https://doi.org/10.1016/j.bcp.2012.10.019> (2013).
16. Antoniadou, I. et al. Novel H₂S-releasing bifunctional antihistamine molecules with improved antipruritic and reduced sedative actions. *J. Med. Chem.* **66**, 9607–9621. <https://doi.org/10.1021/acs.jmedchem.3c00321> (2023).
17. Song, Z.-L. et al. Progress and perspective on hydrogen sulfide donors and their biomedical applications. *Med. Res. Rev.* **42**, 1930–1977. <https://doi.org/10.1002/med.21913> (2022).
18. Gyöngyösi, A. et al. Pharmacological characterization of EV-34, a new H₂S-releasing ibuprofen derivative. *Molecules* **26**, 599–611. <https://doi.org/10.3390/molecules26030599> (2021).
19. Vass, V. et al. Reperfusion-induced injury and the effects of the dithioacetate type hydrogen sulfide donor ibuprofen derivative, BM-88, in isolated rat hearts. *Eur. J. Pharm. Sci.* **185**, 106449–106463. <https://doi.org/10.1016/j.ejps.2023.106449> (2023).
20. Liu, R. & Orgel, L. E. Oxidative acylation using thioacids. *Nature* **389**, 52–54. <https://doi.org/10.1038/37944> (1997).
21. Cerda, M. M. et al. Dithioesters: simple, tunable, cysteine-selective H₂S donors. *Chem. Sci.* **10**, 1773–1779. <https://doi.org/10.1039/C8SC04683B> (2019).
22. Tánzos, B. et al. Effects of H₂S-donor ascorbic acid derivative and ischemia/reperfusion-induced injury in isolated rat hearts. *Eur. J. Pharm. Sci.* **195**, 106721–106736. <https://doi.org/10.1016/j.ejps.2024.106721> (2024).
23. Guinan, M., Benckendorff, C., Smith, M. & Miller, G. J. Recent advances in the chemical synthesis and evaluation of anticancer nucleoside analogues. *Molecules* **25**, 2050–2075. <https://doi.org/10.3390/molecules25092050> (2020).
24. Seley-Radtke, K. L. & Yates, M. K. The evolution of nucleoside analogue antivirals: a review for chemists and non-chemists. Part 1: early structural modifications to the nucleoside scaffold. *Antiviral Res.* **154**, 66–86. <https://doi.org/10.1016/j.antiviral.2018.04.004> (2018).
25. Lougiakakis, N. et al. Synthesis and pharmacological evaluation of novel adenine-hydrogen sulfide slow release hybrids designed as multi-target cardioprotective agents. *J. Med. Chem.* **59**, 1776–1790. <https://doi.org/10.1021/acs.jmedchem.5b01223> (2016).
26. Beltowski, J., Guranowski, A., Jamroz-Wisniewska, A., Wolski, A. & Halas, K. Hydrogen sulfide (H₂S)-mediated vasodilatory effect of nucleoside 5'-monophosphorothioates in perivascular adipose tissue. *Can. J. Physiol. Pharmacol.* **93**, 585–595. <https://doi.org/10.1139/cjpp-2014-0543> (2015).
27. Beltowski, J., Guranowski, A. & Jamroz-Wisniewska, A. Nucleoside monophosphorothioates as the new hydrogen sulfide precursors with unique properties. *Pharmacol. Res.* **81**, 34–43. <https://doi.org/10.1016/j.phrs.2014.01.003> (2014).
28. Zheng, Z. et al. Novel nucleoside-based antimalarial compounds. *Bioorg. Med. Chem. Lett.* **26**, 2861–2865. <https://doi.org/10.1016/j.bmcl.2016.04.053> (2016).
29. Bege, M. et al. In vitro and in vivo antiplasmodial evaluation of sugar-modified nucleoside analogues. *Sci. Rep.* **13**, 12228. <https://doi.org/10.1038/s41598-023-39541-4> (2023).
30. Godoy, A. S. et al. Allosteric regulation and crystallographic fragment screening of SARS-CoV-2 NSP15 endoribonuclease. *Nucleic Acids Res.* **51**, 5255–5270. <https://doi.org/10.1093/nar/gkad314> (2023).
31. Miles, R. W. et al. S-Homoadenosyl-L-cysteine and S-homoadenosyl-L-homocysteine. Synthesis and binding studies of non-hydrolyzed substrate analogues with S-adenosyl-L-homocysteine hydrolase. *J. Org. Chem.* **67**, 8258–8260. <https://doi.org/10.1021/jo020478g> (2002).
32. Bege, M. et al. Synthesis and oligomerization of cysteinyl nucleosides. *Org. Biomol. Chem.* **18**, 8161–8178. <https://doi.org/10.1039/d0ob01890b> (2020).
33. Friedel, H. A., Goa, K. L. & Benfield, P. S-Adenosyl-L-methionine. A review of its pharmacological properties and therapeutic potential in liver dysfunction and affective disorders in relation to its physiological role in cell metabolism. *Drugs* **38**, 389–416. <https://doi.org/10.2165/00003495-198938030-00004> (1989).
34. Bege, M. et al. A low-temperature, photoinduced thiol-ene click reaction: a mild and efficient method for the synthesis of sugar-modified nucleosides. *Org. Biomol. Chem.* **15**, 9226–9233. <https://doi.org/10.1039/C7OB02184D> (2017).
35. Tomasz, J. in *In Nucleic Acid Chemistry Part Two*. 765–769 (eds Townsend, L. B. & Tipson, R. S.) (Wiley, 1978).
36. Kicsák, M. et al. A three-component reagent system for rapid and mild removal of O-, N- and S-trityl protecting groups. *Org. Biomol. Chem.* **14**, 3190–3192. <https://doi.org/10.1039/C6OB00067C> (2016).
37. Debreczeni, N. et al. Tightly linked morpholino-nucleoside chimeras: new, compact cationic oligonucleotide analogues. *Org. Biomol. Chem.* **19**, 8711–8721. <https://doi.org/10.1039/D1OB01174J> (2021).
38. Sugihara, S., Konegawa, N. & Maeda, Y. HCl-Et₂O-Catalyzed metal-free RAFT cationic polymerization: one pot transformation from metal-free living cationic polymerization to RAFT radical polymerization. *Macromolecules* **48**, 5120–5131. <https://doi.org/10.1021/acs.macromol.5b01071> (2015).
39. Gain, C., Song, S., Anguaco, T., Satta, S. & Kelesidis, T. The role of oxidative stress in the pathogenesis of infections with coronaviruses. *Front. Microbiol.* **13**, 1111930. <https://doi.org/10.3389/fmicb.2022.1111930> (2023).
40. Schieber, M. & Chandel, N. S. ROS function in redox signaling and oxidative stress. *Curr. Biol.* **24**, 453–462. <https://doi.org/10.1016/j.cub.2014.03.034> (2015).
41. Shahid, A. & Bhatia, M. Hydrogen sulfide: a versatile molecule and therapeutic target in Health and diseases. *Biomolecules* **14**, 1145. <https://doi.org/10.3390/biom14091145> (2024).
42. Palamara, A. T. et al. Evidence for antiviral activity of glutathione: in vitro inhibition of herpes simplex virus type 1 replication. *Antivir Res.* **27**, 237–253. [https://doi.org/10.1016/0166-3542\(95\)00008-A](https://doi.org/10.1016/0166-3542(95)00008-A) (1995).
43. Hati, S. & Bhattacharyya, S. Impact of thiol-disulfide balance on the binding of Covid-19 spike protein with angiotensin-converting enzyme 2 receptor. *ACS Omega*. **5**, 16292–16298. <https://doi.org/10.1021/acsomega.0c02125> (2020).
44. Manček-Keber, M. et al. Disruption of disulfides within RBD of SARS-CoV-2 spike protein prevents fusion and represents a target for viral entry inhibition by registered drugs. *FASEB J.* **35**, e21651. <https://doi.org/10.1096/fj.202100560R> (2021).
45. Alvarado-Tapias, E. et al. Adenosine induces ventricular arrhythmias in hearts with chronic chagas cardiomyopathy. *Rev. Esp. Cardiol. (Engl Ed)*. **63**, 478–482. [https://doi.org/10.1016/S1885-5857\(10\)70097-9](https://doi.org/10.1016/S1885-5857(10)70097-9) (2010).
46. Guideri, F. et al. QTc interval prolongation during infusion with dipyridamole or adenosine. *Int. J. Cardiol.* **48**, 67–73. [https://doi.org/10.1016/0167-5273\(94\)02209-2](https://doi.org/10.1016/0167-5273(94)02209-2) (1995).
47. Guieu, R. et al. Adenosine and the Cardiovascular System: the good and the bad. *J. Clin. Med.* **9**, 1366. <https://doi.org/10.3390/jcm9051366> (2020).
48. Hori, M. & Kitakaze, M. Adenosine, the heart, and coronary circulation. *Hypertension* **18**, 565–574. <https://doi.org/10.1161/01.HYP.18.5.565> (1991).
49. Liu, X. Y., Qian, L. L. & Wang, R. X. Hydrogen Sulfide-Induced Vasodilation: the involvement of vascular potassium channels. *Front. Pharmacol.* **13**, 911704. <https://doi.org/10.3389/fphar.2022.911704> (2022).
50. Kimura, T., Ho, I. K. & Yamamoto, I. Uridine receptor: Discovery and its involvement in sleep mechanism. *Sleep* **24**, 251–260. <https://doi.org/10.1093/sleep/24.3.251> (2001).
51. Fujisawa, Y. & Mitsunobu, O. Preparation of Deoxyhalogenouridines. *J. Chem. Soc. Chem. Commun.* 201–201. <https://doi.org/10.1039/C39730000201> (1973).
52. Marriotti, J. H., Mottahedeh, M. & Reese, C. B. 9-(4-Methoxyphenyl)xanthen-9-thiol: a useful reagent for the preparation of thiols. *Tetrahedron Lett.* **31**, 7485–7488. [https://doi.org/10.1016/S0040-4039\(00\)88523-8](https://doi.org/10.1016/S0040-4039(00)88523-8) (1990).
53. Shimamura, T. et al. Applicability of the DPPH assay for evaluating the antioxidant capacity of food additives-inter-laboratory evaluation study. *Anal. Sci.* **30**, 717–721. <https://doi.org/10.2116/analsci.30.717> (2014).

54. Szöke, K. et al. Pharmacological evaluation of newly synthesized cannabidiol derivatives on H9c2 cells. *Antioxidants* **12**, 1714–1729. <https://doi.org/10.3390/antiox12091714> (2023).
55. Mosmann, T. Rapid colorimetric assay for cellular growth and survival: application to proliferation and cytotoxicity assays. *J Immunol. Methods*. 65, 55–63. [https://doi.org/10.1016/0022-1759\(83\)90303-4](https://doi.org/10.1016/0022-1759(83)90303-4) (1983).
56. Vecsernyes, M. et al. Alpha-melanocyte-stimulating hormone induces Vasodilation and exerts Cardioprotection through the Heme-Oxygenase Pathway in Rat hearts. *J. Cardiovasc. Pharmacol.* **69**, 286–297. <https://doi.org/10.1097/FJC.0000000000000472> (2017).
57. Percie du Sert et al. The ARRIVE guidelines 2.0: updated guidelines for reporting animal research. *PLoS Biol.* **18** (7), e3000410. <https://doi.org/10.1371/journal.pbio.3000410> (2020).

Acknowledgements

This research was conducted with the support of the National Academy of Scientist Education Program of the National Biomedical Foundation under the sponsorship of the Hungarian Ministry of Culture and Innovation. Chemical synthesis work was funded by the National Research, Development and Innovation Office of Hungary (K 132870 and FK 142315) and by the University of Debrecen Scientific Research Bridging Fund (DETKA). The research was also supported by the EU and co-financed by the European Regional Development Fund under the project GINOP-2.3.4-15-2020-00008. Antiviral tests were funded by the project National Institute Virology and Bacteriology (Programme EXCELES, Project No. LX22NPO5103) - Funded by the European Union - Next Generation EU.

Author contributions

Synthesis of the compounds: M.B. and M.L. NMR characterization: M.B. MALDI characterization and H₂S releasing measurements: I.B. Antiviral assays: J.H. and J.W. DPPH antioxidant assay: R.G.K. ABTS and MTT assays: I.L, R.K. and S.E. HPLC measurements: L. N. In vivo experiments: D.P. and B.B. Conceptualisation and supervision: A.B. and P.H. The main manuscript text was written by M.B., R.G.K., D.P., J.W. and A.B. All authors reviewed the manuscript and all authors have given approval to the final version of the manuscript.

Funding

Open access funding provided by University of Debrecen.

Declarations

Competing interests

The authors declare no competing interests.

Additional information

Supplementary Information The online version contains supplementary material available at <https://doi.org/10.1038/s41598-025-85351-1>.

Correspondence and requests for materials should be addressed to M.B. or A.B.

Reprints and permissions information is available at www.nature.com/reprints.

Publisher's note Springer Nature remains neutral with regard to jurisdictional claims in published maps and institutional affiliations.

Open Access This article is licensed under a Creative Commons Attribution 4.0 International License, which permits use, sharing, adaptation, distribution and reproduction in any medium or format, as long as you give appropriate credit to the original author(s) and the source, provide a link to the Creative Commons licence, and indicate if changes were made. The images or other third party material in this article are included in the article's Creative Commons licence, unless indicated otherwise in a credit line to the material. If material is not included in the article's Creative Commons licence and your intended use is not permitted by statutory regulation or exceeds the permitted use, you will need to obtain permission directly from the copyright holder. To view a copy of this licence, visit <http://creativecommons.org/licenses/by/4.0/>.

© The Author(s) 2025